



Review of the strain-based formulation for analysis of plane structures

Part I: Formulation of basics and the existing elements

M. Rezaiee-Pajand*, N. Gharaei-Moghaddam and M. Ramezani

Abstract

Since the introduction of the finite element approach, as a numerical solution scheme for structural and solid mechanics applications, various formulation methodologies have been proposed. These ways offer different advantages and shortcomings. Among these techniques, the standard displacement-based approach has attracted more interest due to its straightforward scheme and generality. Investigators have proved that the other strategies, such as the force-based, hybrid, assumed stress, and assumed strain provides special advantages in comparison with the classic finite elements. For instance, the mentioned techniques are able to solve difficulties, like shear locking, shear parasitic error, mesh sensitivity, poor convergence, and rotational dependency. The main goal of this two-part study is to present a brief yet clear portrait of the basics and advantages of the direct strain-based method for development of high-performance plane finite elements. In this article, which is the first part of this study, assumptions and the basics of this method are introduced. Then, a detailed review of all the existing strain-based membrane elements is presented. Although the strain formulation is applicable for different types of structures, most of the existing elements pertain to the plane structures. The second part of this study deals with the application and performance of the reviewed elements in the analysis of plane stress/strain problems.

AMS subject classifications (2020): 74K15, 74G15.

*Corresponding author

Received 25 October 2020; revised 8 June 2021; accepted 9 June 2021

Mohammad Rezaiee-Pajand

Professor of Civil Engineering, School of Engineering, Ferdowsi University of Mashhad, Iran. e-mail: Rezaiee@um.ac.ir, Tel/fax: +98-51-38412912

Nima Gharaei-Moghaddam

PhD of Structural Engineering, School of Engineering, Ferdowsi University of Mashhad, Iran. e-mail: Nima.Gharaei@gmail.com, Tel: +98-915-1589342

Mohammadreza Ramezani

PhD Student of Structural Engineering, School of Engineering, Ferdowsi University of Mashhad, Iran. e-mail: Mohammadrezaramezani1994@gmail.com, Tel: +98-915-1076010

Keywords: Strain-based formulation; Higher-order strain field; Equilibrium condition; Numerical evaluation; Drilling degrees of freedom.

1 Introduction

Numerical methods are proved to be powerful and effective computational tools for analysis of complicated and practical engineering problems. According to different features of scientific activities and in demand of special requirements, many diverse numerical techniques are developed in the past decades, such as the finite element method, finite difference technique, boundary element method, and discrete element approach. Each of these various numerical methods have their own advantages and shortcomings, but the finite element methods gain more popularity due to their strong mathematical bases and inherent capabilities, which result in increasing application of this scheme in different fields of science and especially engineering fields [5, 6, 28, 39, 40, 42, 43, 78, 79]. Therefore, various formulation techniques are developed in the past decades and there are thousands of finite elements available for analysis of dissimilar types of problems and structures [8, 13, 21, 22, 41, 53].

Among the available approaches for finite element formulation, the most well-known and widely applicable one is the displacement-based technique. This method, which sometimes is called with different terms, such as, the classical or stiffness approach, is the first scheme that was used for the development of finite elements; see [80]. Clear and straightforward process and applicability to different types of problems and structures are the prominent advantages of the displacement-based formulation for structural and mechanical applications. However, this process has various shortcomings. For instance, inaccuracy and discontinuity of stresses, which are secondary parameters in stiffness approach, are a vital deficiency in structural applications, where stress is a decisive parameter in the design practice; see [33, 52]. It should be noted that this problem can partly be solved by using higher order formulations, which leads to the application of internal nodes, and increases computational costs, and reduces the numerical efficiency of the analysis [23, 36, 54, 55]. Another common problem of displacement-based finite elements in various locking phenomena, such as, shear and membrane locking, which necessitate special treating, which sometimes requires considerable time and effort and reduces the efficiency of the method [54, 55]. Moreover, in severely nonlinear problems, the displacement-based elements usually necessitate utilization of very fine meshes, which is inappropriate from the efficiency standpoint [46, 47, 74]. To remedy the mentioned and other shortcomings of the displacement approach, other finite element formulations, such as the force-based, hybrid or mixed, assumed stress, and assumed strain has been developed. Fortunately, these new procedures have

their own advantages and shortcomings. For example, the force-based formulation performs very well in the linear and nonlinear analysis of frame structures and also provides an appropriate platform for the development of advanced frame elements [3, 34, 56, 57, 73, 76]. It is reminded that the force formulation approach is limited to skeletal structures and that its application for continuous structures is very difficult if not impossible.

Although each method has different merits and limitations, some of the approaches have received more attention from researchers, while the others have remained less treated. One of these techniques that has received less attention despite its promising performance, is the strain-based or assumed strain approach [17, 25, 35, 38]. Therefore, the main purpose of this study is to introduce basics of the strain-based formulation. The strain formulation method can be classified in three distinct groups, namely free formulation, assumed natural strain method, and direct approach.

The free formulation method is based on the kinematic decomposition, in which the element displacements are decomposed in two basic and higher-order parts [25, 38]. The basic part represents the rigid body motions and constant strain state, which is necessary for the convergence criteria. On the other hand, the higher-order terms improve accuracy of the finite element by establishing proper rank of the stiffness matrix. The conditions of force and energy orthogonality result in the algebraic formulation of the stiffness matrix, which satisfies the individual element test. It is noteworthy that the strain functions in this method are dependent on displacements one; see [19]. The second method for the development of strain-based elements is the assumed natural deviatoric strain (ANDES) approach [27]. In this technique, the independent strain function is applied, which includes basic and higher-order parts. The deviation of strain from the constant strain is represented by the higher-order part of the strain function. In this way, the higher-order part is selected so that the integral of higher-order strain through the element equals zero. Therefore, *ANDES* technique satisfies the individual element test [27].

The third method is the direct formulation approach, in which Taylor series for the strain field is used to approximate the strain field [63]. The resulting elements from this approach lead free from the shear locking and parasitic shear error. The strain states in this approach can be divided into rigid body motions, constant strain, and higher-order strain states. The rigid body modes and constant strain states guarantee the convergence of resulting element. The higher-order terms have a parametric form that can be optimized to obtain efficient elements. The optimization is performed by enforcing different optimal conditions. Some of these optimal conditions will be discussed in the coming sections. It is important to note that the optimization process of the finite element templates is a relatively complicated task that requires innovation [63].

As mentioned, the strain-based formulation itself can be categorized in three different subdivisions. In this study, only the direct method is covered.

After the presentation of the formulation basics, a detailed review of the existing assumed-strain membrane elements is presented. This article is the first part of a two-part study. In the second part, numerical comparison of the reviewed elements is performed. This article is organized in the following order: Section 2 presents basis steps for the development of the plane elements with the assumed strain approach. Other important optimal criteria for assumed strain elements are introduced in Section 3. The existing triangular membrane elements are reviewed in Section 4, and Section 5 discusses the available quadrilateral plane elements. In Section 6, some of the accessible strain-based elements for the other types of structures are briefly introduced. Finally, Section 7 presents the concluding remarks of the article.

2 Basics of the formulation

In the assumed strain formulation, the element strain field is approximated by an assumed mathematical function. As mentioned, like any other form of the finite element formulation, there are different types of assumed strain formulation [4, 20, 26, 37]. However, in this study, only the direct strain-based formulation will be discussed [63]. The following formulation steps pertain to development of plane finite elements. Needless to say, the presented process can be simply applied to the other types of elements with only slight modifications. The main reasons behind narrowing the scope of the present review are the availability of the relatively large number of existing strain-based elements developed based on the various types of strain-based formulation. These researches made the current study very lengthy. Moreover, the growing interest from the structural analysis community toward the direct method in recent years, and also the valuable experiences of the authors in this field, which should be exposed to the younger analysts.

In the case of plane problems, the strain field consists of three components, namely ε_x , ε_y , and γ_{xy} . Based on the Taylor expansion, each function can be approximated by a polynomial function of arbitrary order. Therefore, the strain components are approximated as follows:

$$\begin{cases} \varepsilon_x(x, y) = (\varepsilon_x)_o + (\varepsilon_{x,x})_o x + (\varepsilon_{x,y})_o y + (\varepsilon_{x,xx})_o \left(\frac{x^2}{2}\right) + (\varepsilon_{x,xy})_o (xy) + (\varepsilon_{x,yy})_o \left(\frac{y^2}{2}\right) + \dots, \\ \varepsilon_y(x, y) = (\varepsilon_y)_o + (\varepsilon_{y,x})_o x + (\varepsilon_{y,y})_o y + (\varepsilon_{y,xx})_o \left(\frac{x^2}{2}\right) + (\varepsilon_{y,xy})_o (xy) + (\varepsilon_{y,yy})_o \left(\frac{y^2}{2}\right) + \dots, \\ \gamma_{xy}(x, y) = (\gamma_{xy})_o + (\gamma_{xy,x})_o x + (\gamma_{xy,y})_o y + (\gamma_{xy,xx})_o \left(\frac{x^2}{2}\right) + (\gamma_{xy,xy})_o (xy) + (\gamma_{xy,yy})_o \left(\frac{y^2}{2}\right) + \dots \end{cases} \quad (1)$$

Here “,” indicates differentiating with respect to its following variable. Moreover, the subscript “o” indicates the value of the strain gradient at the origin of the coordinate system. The coefficients with the subscript “o” are called strain states. Selection of diverse polynomials with a different number of terms and various orders results in finite elements with a different number of degrees of freedom, as well as, the specific properties. Due to the importance of the constant strain states for the convergence of the resulting finite

element, the selection of the constant and linear terms for strain components is necessary. Selection of the higher-order terms would increase the accuracy and the convergence rate of the resulting finite element, but instead reduces its numerical efficiency. As it was mentioned previously, it is possible to apply different optimal criteria, such as pure plain bending test, for improving performance of the resulting finite element. However, such optimal conditions are optional, and the only necessity is to include the constant terms in the opted assumed strain field. However, similar to the classical formulation, it is suggested not to give any priority to each of the coordinates, (x or y). In addition, if the analytical estimation of the strain field is available, then the terms of the approximated field can be selected based on the known analytical solution.

Nevertheless, after choosing the desired terms, the assumed strain field can be optimized by applying any desired optimal condition [38, 63, 71]. The most common criteria are compatibility and equilibrium conditions [63, 71]. The compatibility of the strain field is achieved provided that the next relationship exists between the strain components [71]:

$$\frac{\partial^2 \varepsilon_x}{\partial y^2} + \frac{\partial^2 \varepsilon_y}{\partial x^2} = \frac{\partial^2 \gamma_{xy}}{\partial x \partial y}. \quad (2)$$

It is obvious that in the general case, for the satisfaction of the compatibility or any other criteria; it might be needed that some strain states be dependent on each other. Therefore, imposing the optimized condition results in the dependency of some strain states to each other and therefore, it reduces the number of independent strain states [27]. As it will be shown later, the number of independent strain states is equal to the number of required degrees of freedom for the element.

The other conventional optimal condition is the equilibrium. It was proved that if the equilibrium equation is satisfied within an element, then it can be included in the Trefftz formulation [27]. The equation of equilibrium for the plane problems is defined as follows:

$$\begin{cases} \frac{\partial \sigma_x}{\partial x} + \frac{\partial \tau_{xy}}{\partial y} + F_x = 0, \\ \frac{\partial \sigma_y}{\partial y} + \frac{\partial \tau_{xy}}{\partial x} + F_y = 0, \end{cases} \quad (3)$$

where F_x and F_y are the body forces in the x and y directions, respectively. Also, σ_x , σ_y and τ_{xy} are normal and shearing stresses, respectively. To rewrite the equilibrium equation in terms of strain, it is necessary to relate the stresses to the strains. For the plane problems, the coming relations connect stresses and strains:

$$\begin{cases} \sigma_x = 2G\varepsilon_x + \lambda(\varepsilon_x + \varepsilon_y), \\ \sigma_y = 2G\varepsilon_y + \lambda(\varepsilon_x + \varepsilon_y), \\ \tau_{xy} = G\gamma_{xy}. \end{cases} \quad (4)$$

In the previous equations, G and ν are the shear modulus and Poisson's ratio, respectively. Indeed λ is called the Lamé constant and is equal to $\frac{\nu E}{(1+\nu)(1-2\nu)}$ for the plane stress condition. In the case of plane strain, this constant is equal to $\frac{\nu E}{(1+\nu)(1-2\nu)}$. Here, E stands for modulus of elasticity. Substituting equations (4) in the equilibrium equation results in the following relations:

$$\begin{cases} (2G + \lambda) \frac{\partial \varepsilon_x}{\partial x} + \lambda \frac{\partial \varepsilon_y}{\partial x} + G \frac{\partial \gamma_{xy}}{\partial y} + F_x = 0, \\ \lambda \frac{\partial \varepsilon_x}{\partial y} + (2G + \lambda) \frac{\partial \varepsilon_y}{\partial y} + G \frac{\partial \gamma_{xy}}{\partial x} + F_y = 0. \end{cases} \quad (5)$$

It is noteworthy that imposing the optimized conditions, such as; compatibility and equilibrium, is not necessary steps for developing a plane element based on assumed strain approach, and as it will be shown in the coming section, there are finite elements, which do not consider these criteria [71, 72]. However, enforcing these conditions to the assumed strain field improves the performance of the resulting element. As mentioned previously, the inclusion of the optimized condition makes some of the strain states to be depended on the other ones. When the dependent strain states are determined, the assumed strain field is rewritten in terms of the independent ones. The next step is to calculate the associated displacement field. For this purpose, the strain-displacement formulas are utilized:

$$\begin{cases} \varepsilon_x = \frac{\partial u}{\partial x}, \\ \varepsilon_y = \frac{\partial v}{\partial y}, \\ \gamma_{xy} = \frac{1}{2} \left(\frac{\partial u}{\partial y} + \frac{\partial v}{\partial x} \right). \end{cases} \quad (6)$$

In these relations, u and v are displacements in the x and y directions, respectively. Based on these qualities, the displacements in x and y directions are derived by integrating normal strain components with respect to their associated coordinates:

$$\begin{cases} u(x, y) = \int \varepsilon_x dx + f_1(y), \\ v(x, y) = \int \varepsilon_y dy + f_2(x). \end{cases} \quad (7)$$

Here, f_1 and f_2 are the results of integrating shear strain with respect to the coordinates and imposing the rigid body modes condition. In the case of plane problems, three rigid body modes exist in the displacement field, namely u_o , v_o , and r_o , signifying the rigid body displacements in x and y directions and the rigid body rotation, respectively. As it was mentioned, the existence of these terms is the necessary convergence condition. Accordingly, these modes are also counted among the independent strain states that can be arranged in a vector arrangement indicated by S . This vector is called strain state vector, which consists of the independent strain states. They are the coefficients of the strain field approximations in (1), as well as, the rigid body modes. The strain state vector is somehow equivalent to the

nodal displacement vector in the traditional displacement-based approach. By using the matrix notation, which is traditionally used in finite element formulation in structural engineering applications, it is possible to relate the displacement and strain fields to the strain state vector in the subsequent forms:

$$U = N_s S + \tilde{U}, \quad (8)$$

$$\varepsilon = B_s S + \tilde{\varepsilon}. \quad (9)$$

In these equations, N_s and B_s represent the displacement and strain interpolation matrices, respectively. The particular response of the displacement and strain fields, that is, \tilde{U} and $\tilde{\varepsilon}$, depend on the body forces. The next relation can be established between the vectors of nodal displacements and the strain states:

$$D = AS + \tilde{D} = \bar{D} + \tilde{D}. \quad (10)$$

Here, D and \tilde{D} are the nodal displacement vectors and the displacements due to body forces. Also, A is a geometric matrix including of the nodal displacement interpolation matrices. It is possible to construct the subsequent relations between the displacement and strains' fields of the element with the nodal displacement vector using (10) as follows:

$$U = N_s S + \tilde{U} = N_s (A^{-1} \bar{D}) + \tilde{U} = (N_s A^{-1}) \bar{D} + \tilde{U} = N \bar{D} + \tilde{U}, \quad (11)$$

$$\varepsilon = B_s S + \tilde{\varepsilon} = B_s (A^{-1} \bar{D}) + \tilde{\varepsilon} = (B_s A^{-1}) \bar{D} + \tilde{\varepsilon} = B \bar{D} + \tilde{\varepsilon}. \quad (12)$$

Assuming the body forces to be negligible in comparison with the applied external loads, the strains and displacements due to body forces, $\tilde{\varepsilon}$ and \tilde{U} , are neglected.

The final step of the formulation is to derive the element stiffness matrix and the nodal force vector. Among different approaches for this purpose, the minimization of the total potential energy is the most common approach. The total potential energy functional can be established as follows:

$$\Pi = \frac{1}{2} \int \sigma^T \varepsilon dV - \int U^T F dV - D^T P_{ext}. \quad (13)$$

In this equation, P_{ext} and F stand for the external nodal and the body forces, respectively. The element stiffness matrix and nodal force vector are derived by establishing the stationary of the following functional:

$$\frac{\partial \Pi}{\partial \bar{D}} = A^{-T} \left(\int B_s^T D_m B_s dv \right) A^{-1} \bar{D} - A^{-T} \left(\int N_s^T F dv \right) - P_{ext} = K \bar{D} - P = 0. \quad (14)$$

Therefore, the element stiffness matrix and the nodal force vector are derived in the following form:

$$K = A^{-T} \left(\int B_s^T D_m B_s dv \right) A^{-1} = A^{-T} K_0 A^{-1}, \quad (15)$$

$$P = P_{ext} + A^{-T} \left(\int N_s^T F dv \right), \quad (16)$$

where, D_m is the material matrix:

$$D_m = \frac{E}{1 - \nu^2} \begin{bmatrix} 1 & \nu & 0 \\ \nu & 1 & 0 \\ 0 & 0 & \frac{1-\nu}{2} \end{bmatrix}. \quad (17)$$

It is noteworthy that for plane problems, which is the main subject of this study, the volume integral in the above-mentioned equations simply transforms into an area integral considering the constant unit thickness for the plane structures.

3 Required optimal criteria

As mentioned previously, in order to achieve an optimal and efficient formulation, it is possible to impose different criteria on the assumed strain field. Two of these criteria, compatibility and equilibrium, are defined in the previous section. In this section, two other required criteria for the optimal performance of assumed strain elements are defined.

3.1 Pure bending test

To achieve optimal performance in flexural behavior, Felippa [18, 26] utilized the pure bending test. In this experiment, an Euler–Bernoulli beam is discretized by rectangular (or triangular) elements and loaded by the constant bending moments. To study in-plane bending along x and y axes, the two beams depicted in Figures 1 and 2 are considered.

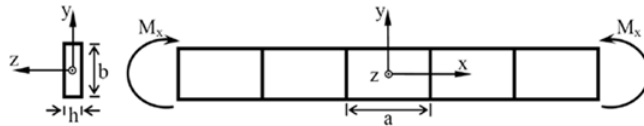
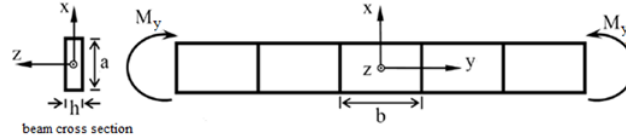


Figure 1: Pure bending test in the xy plane

The stored elastic energy due to the constant moments, M_x and M_y , in part of the beams meshed with one rectangular element (or two triangular elements) is derived according to the following relations:

$$U_x^{exact} = \frac{6aM_x^2}{Eb^3h}, \quad (18)$$

$$U_y^{exact} = \frac{6bM_y^2}{Ea^3h}. \quad (19)$$

Figure 2: Pure bending test in the zy plane

Based on this test, an element can present bending behavior exactly, provided that it can compute precise elastic stored energy. In other words, the ratio of the energy calculated according to the results of element analysis to the exact stored elastic energy should be equal to 1. For this purpose, the element stored energy, based on finite element responses, is computed using the coming equations:

$$U_x^{element} = \frac{1}{2} D_{bx}^T K D_{bx}, \quad (20)$$

$$U_y^{element} = \frac{1}{2} D_{by}^T K D_{by}. \quad (21)$$

In these relations, D_{bx} and D_{by} are the nodal displacement vector of the element and K is the element stiffness matrix. Therefore, the previously mentioned flexural energy ratios are derived as follows:

$$r_x = \frac{U_x^{element}}{U_x^{exact}}, \quad (22)$$

$$r_y = \frac{U_y^{element}}{U_y^{exact}}. \quad (23)$$

If r_x or r_y is equal to 1, the element passes the pure bending test and is able to represent exact bending behavior. If these ratios are greater or less than 1, then the element is over-stiff or over-flexible, respectively. Moreover, if the energy ratios are equal to 1 for any aspect ratio (a/b), then the element is optimal in bending behavior. Finally, the element suffers from shear locking on the condition that $a \gg b$ results in $r_x \gg 1$ or if $b \gg a$ leads to $r_y \gg 1$.

To study this test for the strain-based formulation, it is required to investigate the exact strain fields of the elements under pure bending. In the following, only the case of M_x will be discussed. The same reasoning goes for M_y , as well. The exact stress components of the beam subjected to the

pure bending M_x are as follows:

$$\begin{cases} \sigma_x = -\frac{12M_x y}{b^3 h}, \\ \sigma_y = 0, \\ \tau_{xy} = 0. \end{cases} \quad (24)$$

Therefore, the element stress field can be demonstrated by the linear function of y for σ_x in the subsequent form:

$$\begin{cases} \sigma_x = \alpha_1 + \alpha_2 y, \\ \sigma_y = 0, \\ \tau_{xy} = 0. \end{cases} \quad (25)$$

Based on the Hook's law, the corresponding strain field is as follows:

$$\begin{cases} \varepsilon_x = \frac{\alpha_1}{E} + \frac{\alpha_2}{E} y = \beta_1 + \beta_2 y, \\ \sigma_y = \frac{-\nu\alpha_1}{E} - \frac{\nu\alpha_2}{E} y = \beta_3 + \beta_4 y, \\ \tau_{xy} = 0. \end{cases} \quad (26)$$

From the previous relations, it can be concluded that a strain-based element would surely pass the pure bending test, provided that the constant and linear terms for the normal strains are included in the assumed strain field.

3.2 Rotational invariance

Because the finite elements may be rotated with the different angles and be placed in various locations in the structural meshes used for the analysis of the diverse problems, their characteristics must not change due to the rotation. Such an element is called a rotational invariant. Assuming that the coordinate system xy is rotated to a new form, which is indicated by $x'y'$. The displacements' components in this new coordinate system can be related to those of the initial coordinate system by using the following simple transformations:

$$u' = u \cos \theta + v \sin \theta, \quad (27)$$

$$v' = -u \sin \theta + v \cos \theta. \quad (28)$$

In this relation, θ is the rotation angle from xy system to the new $x'y'$ coordinates. Based on this relation, having the rigid body motions, u_0 and v_0 in the original coordinate, it is possible to calculate the correct value of u'_0 and v'_0 , in the $x'y'$ coordinates, by using equations (27) and (28). Regarding the rotational invariance property, it is required to consider the strain field with

a complete order. In other words, some incomplete interpolation polynomials produce strain states that are not invariant with rotation. Therefore, the rotational invariance can be guaranteed with the inclusion of all strain terms with a given order. For instance, the rotational mapping of a constant strain state is as follows:

$$\varepsilon'_x = \varepsilon_x \cos^2 \theta + \varepsilon_y \sin^2 \theta + \gamma_{xy} \sin \theta \cos \theta , \quad (29)$$

$$\varepsilon'_y = \varepsilon_x \sin^2 \theta + \varepsilon_y \cos^2 \theta - \gamma_{xy} \sin \theta \cos \theta , \quad (30)$$

$$\gamma'_{xy} = (\varepsilon_x - \varepsilon_y) \sin 2\theta + \gamma_{xy} \cos 2\theta . \quad (31)$$

Based on these relations, a strain-based element can represent the constant strains with respect to any system of the coordinates, only on the condition that its formulation takes into account all three cases of the constant strain states. Although, the completeness of the assumed strain field guarantees rotational invariance of the element, the elements with incomplete strain fields are not necessarily rotational dependent.

4 Triangular membrane elements

To the author's best knowledge, there are thirteen strain-based triangular elements formulated by using direct strain-based formulation. In this section, thirteen triangular membrane elements proposed based on the assumed-strain approach are briefly reviewed. These studies are arranged in historical order. Most of the available triangular element has similar geometry, a three-node triangle with three degrees of freedom at each node. However, in this configuration, the incorporation of the drilling degrees of freedom improves the performance of the element in bending analysis, but more recent works utilized different distribution of degrees of freedom provide better results. In addition, as it will be demonstrated, in the most of the existing elements, the equilibrium conditions are not imposed on the assumed strain fields. According to the outcomes of the more recent elements, considering the equilibrium conditions improve the accuracy and convergence rate of the suggested strain-based elements. More details about these elements are provided in the following descriptions. To facilitate understanding and reproducing of the elements by readers, the main details are presented in a table format.

4.1 Sabir (1985)

The first researcher that utilized the assumed strain approach to develop more powerful membrane elements is Sabir. In one of his early works, he [71] proposed a three-node triangular element with three-degrees of freedom at

each node. The assumed strain components satisfied the compatibility equation, but the equilibrium equations were not satisfied. The drilling degree of freedom for the element was defined by the subsequent relation:

$$\theta = \frac{1}{2} \left(\frac{\partial v}{\partial x} - \frac{\partial u}{\partial y} \right). \quad (32)$$

Details of the element formulation are presented in Table 1.

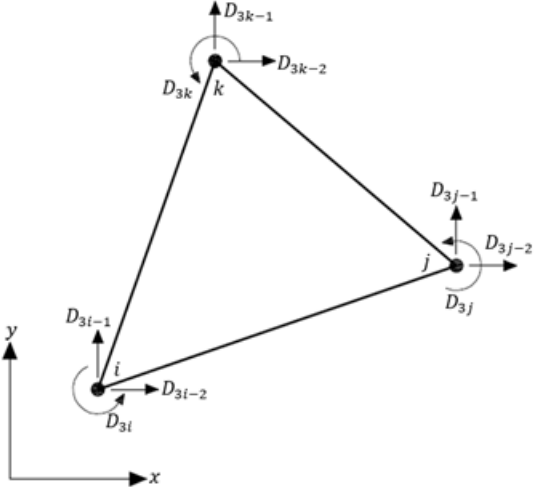
4.2 Sabir and Sfindji (1995)

Sabir and Sfindji [72] suggested a four-node triangular element by assumption of the linear normal strains and constant shear strain. The selected strain field satisfied the compatibility condition, but the equilibrium equations were not imposed on this strain field. Therefore, the strain state vector consisted of eight independent unknown coefficients. Three nodes were located at the vertexes of the triangle, and the fourth node was placed in the middle of one side. Each node had two translational degrees of freedom. Consequently, the element possessed eight degrees of freedom totally. This geometry made the element appropriate to be used as transitional element in finite element meshes. They compared the performance of their suggested element with standard displacement-based element by using few simple numerical problems [72]. Their attained results showed better performance of this triangular strain-based element. Table 2 presents details of this element.

4.3 Tayeh (2003)

In 2003, Tayeh [75] developed new strain-based elements for analysis of the plane structures. In contrast to the previous works by Sabir, he utilized higher-order terms and assumed an incomplete second-order field for the element (see Table 3). It is evident that some coefficients in this assumed strain field are common between different strain components. Tayeh provided no clear reason for this selection, but he stated indirectly that this strain field was selected in order to satisfy the compatibility condition. Similar to the element proposed by Sabir and Sfindji [72], the assumed strain field did not satisfy equilibrium equations.

Table 1: Details of the triangular element proposed by Sabir [71]

Ref	Properties	Geometry
Sabir [71]	Geometry	
	Strain field	$\begin{cases} \varepsilon_x(x, y) = (\varepsilon_x)_o + (\varepsilon_{x,y})_o y + (\varepsilon_{y,x})_o x \\ \varepsilon_y(x, y) = (\varepsilon_y)_o + (\varepsilon_{y,x})_o x + (\varepsilon_{x,y})_o y \\ \gamma_{xy}(x, y) = (\gamma_{xy})_o + (\gamma_{xy,x})_o x + (\gamma_{xy,y})_o y \end{cases}$
	Strain state vector	$S = \{u_o \quad v_o \quad r_o \quad (\varepsilon_x)_o \quad (\varepsilon_y)_o \quad (\gamma_{xy})_o \quad (\varepsilon_{x,y})_o \quad (\varepsilon_{y,x})_o \quad (\gamma_{xy,x})_o\}^T$
	Nodal displacement vector	$D = \{D_{3i-2} \quad D_{3i-1} \quad D_{3i} \quad D_{3j-2} \quad D_{3j-1} \quad D_{3j} \quad D_{3k-2} \quad D_{3k-1} \quad D_{3k}\}^T$
	Strain interpolation matrix	$B_s = \begin{bmatrix} 0 & 0 & 0 & 1 & 0 & 0 & y & x & 0 \\ 0 & 0 & 0 & 0 & 1 & 0 & y & x & 0 \\ 0 & 0 & 0 & 0 & 0 & 1 & 0 & 0 & x + y \end{bmatrix}$
	Displacement interpolation matrix	$N_s = \begin{bmatrix} 1 & 0 & -y & x & 0 & \frac{y}{2} & xy & \frac{x^2-y^2}{2} & \frac{y^2}{2} \\ 0 & 1 & x & 0 & y & \frac{x}{2} & \frac{y^2-x^2}{2} & xy & \frac{x^2}{2} \\ 0 & 0 & 1 & 0 & 0 & 0 & -x & y & \frac{x-y}{2} \end{bmatrix}$
	Geometric matrix	$A = [N_{si} \quad N_{sj} \quad N_{sk}]^T$

4.4 Belarbi and Bourezane (2005-first triangular element)

As mentioned previously, most of the available triangular strain-based plane elements have the geometry similar to the one in Table 1. In fact, many of these elements attempted to improve the performance of element suggested

Table 2: Details of the triangular element proposed by Sabir and Sfindji [72]

Ref	Properties	Geometry
Sabir and Sfindji [72]	Geometry	
	Strain field	$\begin{cases} \varepsilon_x(x, y) = (\varepsilon_x)_o + (\varepsilon_{x,y})_o y \\ \varepsilon_y(x, y) = (\varepsilon_y)_o + (\varepsilon_{y,x})_o x \\ \gamma_{xy}(x, y) = (\gamma_{xy})_o \end{cases}$
	Strain state vector	$S = \{u_o \quad v_o \quad r_o \quad (\varepsilon_x)_o \quad (\varepsilon_y)_o \quad (\gamma_{xy})_o \quad (\varepsilon_{x,y})_o \quad (\varepsilon_{y,x})_o\}^T$
	Nodal displacement vector	$D = \{D_{2i-1} \quad D_{2i} \quad D_{2j-1} \quad D_{2j} \quad D_{2k-1} \quad D_{2k} \quad D_{2l-1} \quad D_{2l}\}^T$
	Strain interpolation matrix	$B_s = \begin{bmatrix} 0 & 0 & 0 & 1 & 0 & 0 & y & 0 \\ 0 & 0 & 0 & 0 & 1 & 0 & 0 & x \\ 0 & 0 & 0 & 0 & 0 & 1 & 0 & 0 \end{bmatrix}$
	Displacement interpolation matrix	$N_s = \begin{bmatrix} 1 & 0 & -y & x & 0 & \frac{y}{2} & xy & -\frac{y^2}{2} \\ 0 & 1 & x & 0 & y & \frac{x}{2} & -\frac{x^2}{2} & xy \end{bmatrix}$
	Geometric matrix	$A = [N_{si} \quad N_{sj} \quad N_{sk} \quad N_{sl}]^T$

by Sabir [71]. In one of these research works, Belarbi and Bourezane [9] proposed a new element by incorporating Poisson’s ratio in the assumed strain field. They suspected that unsatisfactory performance of the element proposed by Sabir might be due to the existence of coupling terms in the direct strains. Therefore, they included the Poisson’s ratio in their assumed strain-field (see Table 4). Like the previous strain-based triangular elements, the utilized strain field in this study satisfied the compatibility condition, but the equilibrium equations were not considered in this formulation.

Table 3: Details of the triangular element proposed by Tayeh [75]

Ref	Properties	Geometry
Tayeh [75]	Geometry	Same as Table 1
	Strain field	$\begin{cases} \varepsilon_x(x, y) = (\varepsilon_x)_o + (\varepsilon_{x,y})_o y + (\varepsilon_{x,yy})_o \frac{y^2}{4} \\ \varepsilon_y(x, y) = (\varepsilon_y)_o + (\varepsilon_{y,x})_o x - (\varepsilon_{x,yy})_o \frac{x^2}{4} \\ \gamma_{xy}(x, y) = (\gamma_{xy})_o + (\varepsilon_{y,xx})_o x + (\varepsilon_{y,xx})_o y \\ -(\varepsilon_{x,y})_o \frac{x^2}{4} + (\varepsilon_{y,x})_o \frac{y^2}{4} \end{cases}$
	Strain state vector	$S = \{u_o \quad v_o \quad r_o \quad (\varepsilon_x)_o \quad (\varepsilon_y)_o \quad (\gamma_{xy})_o \quad (\varepsilon_{x,y})_o \quad (\varepsilon_{y,x})_o \quad (\varepsilon_{x,yy})_o\}^T$
	Nodal displacement vector	Same as Table 1
	Strain interpolation matrix	$B_s = \begin{bmatrix} 0 & 0 & 0 & 1 & 0 & 0 & y & 0 & \frac{y^2}{4} \\ 0 & 0 & 0 & 0 & 1 & 0 & 0 & x & -\frac{x^2}{4} \\ 0 & 0 & 0 & 0 & 0 & 1 & -\frac{x^2}{4} & \frac{y^2}{4} & x + y \end{bmatrix}$
	Displacement interpolation matrix	$N_s = \begin{bmatrix} 1 & 0 & -y & x & 0 & \frac{y}{2} & xy & \frac{y^3}{12} - \frac{y^2}{2} & \frac{xy^2}{4} + \frac{y^2}{2} \\ 0 & 1 & x & 0 & y & \frac{x}{2} & -\frac{x^3}{12} - \frac{x^2}{2} & xy & \frac{x^2}{2} - \frac{x^2 y}{4} \\ 0 & 0 & 1 & 0 & 0 & 0 & -\frac{x^2}{8} - x & -\frac{y^2}{8} + y & \frac{x}{2} - \frac{y}{2} - \frac{xy}{2} \end{bmatrix}$
	Geometric matrix	Same as Table 1

4.5 Belarbi and Bourezane (2005- second triangular element)

In 2005, Belarbi and Bourezane [10] performed another study and proposed a triangular strain-based element with the geometry similar to their previous work, but with a different strain field. They assumed linear variation of normal strain with respect to the perpendicular direction for this element, while the incomplete second-order field was assumed for shear strain. Once again, the three-node nine-degrees of freedom geometry was considered for this element. Further details of the element are provided in Table 5.

4.6 Rezaiee-Pajand and Yaghoobi (2014- first triangular element)

Rezaiee-Pajand and Yaghoobi [65] proposed a five-node triangular element with a complete linear strain field, which its geometry and details are presented in Table 6.

In the assumed strain field, there are nine strain states and three rigid body modes, which totally become twelve strain states. The selected strain

Table 4: Details of the first triangular element proposed by Belarbi and Bourezane [9]

Ref	Properties	Geometry
Belarbi and Bourezane [9]	Geometry	Same as Table 1
	Strain field	$\begin{cases} \varepsilon_x(x, y) = (\varepsilon_x)_o + (\varepsilon_{x,y})_o y - (\varepsilon_{x,x})_o x \frac{1-\nu}{2} \\ -(\varepsilon_{y,x})_o x \nu \\ \varepsilon_y(x, y) = (\varepsilon_y)_o + (\varepsilon_{y,x})_o x - (\varepsilon_{x,x})_o y \frac{1-\nu}{2} \\ -(\varepsilon_{x,y})_o y \nu \\ \gamma_{xy}(x, y) = (\gamma_{xy})_o + (\varepsilon_{x,x})_o x + (\varepsilon_{x,x})_o y \end{cases}$
	Strain state vector	$S = \{u_o \quad v_o \quad r_o \quad (\varepsilon_x)_o \quad (\varepsilon_y)_o \quad (\gamma_{xy})_o \quad (\varepsilon_{x,y})_o \quad (\varepsilon_{y,x})_o \quad (\varepsilon_{x,x})_o\}^T$
	Nodal displacement vector	Same as Table 1
	Strain interpolation matrix	$B_s = \begin{bmatrix} 0 & 0 & 0 & 1 & 0 & 0 & y & -\nu x & \frac{-\nu x}{2} \\ 0 & 0 & 0 & 0 & 1 & 0 & -\nu y & x & \frac{-\nu y}{2} \\ 0 & 0 & 0 & 0 & 0 & 1 & 0 & 0 & x + y \end{bmatrix}$
	Displacement interpolation matrix	$N_s = \begin{bmatrix} 1 & 0 & -y & x & 0 & \frac{y}{2} & xy & -\frac{y^2}{2} & -\frac{\nu x^2}{2} & \frac{y^2}{2} & -\frac{\nu x^2}{4} \\ 0 & 1 & x & 0 & y & \frac{x}{2} & -\frac{x^2}{2} & -\frac{\nu y^2}{2} & xy & \frac{x^2}{2} & -\frac{\nu y^2}{4} \\ 0 & 0 & 1 & 0 & 0 & 0 & -x & y & y & \frac{x-y}{2} \end{bmatrix}$
	Geometric matrix	Same as Table 1

components satisfy the compatibility requirement. In addition, Rezaiee-Pajand and Yaghoobi enforced equilibrium conditions in this strain field. They found that the necessary condition for satisfaction of the equilibrium criteria is that some strain states be dependent to others. Therefore, they selected the two dependent strain states, and as a result; ten independent strain states remained. In agreement with the number of independent strain states, the resulting element needs ten degrees of freedom. Rezaiee-Pajand and Yaghoobi considered a triangular element with six nodes, as depicted in Table 6. It is evident, four of these nodes have two translational degrees of freedom, while the other two only have one translational degree of freedom perpendicular to the corresponding side of the element.

The displacements of mid-side nodes, which are perpendicular to the element sides, can be connected to the displacements of the nodes in x and y direction, by using the following relationship:

$$w = u \cdot \sin(\alpha) + v \cdot \cos(\alpha). \tag{33}$$

In which, α is the angle between the degree of freedom normal to the side and the x axis. In this case, due to the difference in the number of degrees of freedom at the nodes, the geometrical matrix is a bit dissimilar to the

Table 5: Details of the second triangular element proposed by Belarbi and Bourezane [10]

Ref	Properties	Geometry
Belarbi and Bourezane [10]	Geometry	Same as Table 1
	Strain field	$\begin{cases} \varepsilon_x(x, y) = (\varepsilon_x)_o + (\varepsilon_{x,y})_o y \\ \varepsilon_y(x, y) = (\varepsilon_y)_o + (\varepsilon_{y,x})_o x \\ \gamma_{xy}(x, y) = (\gamma_{xy})_o + (\gamma_{xy,xx})_o x^2 + (\gamma_{xy,xx})_o y^2 \end{cases}$
	Strain state vector	$S = \{u_o \quad v_o \quad r_o \quad (\varepsilon_x)_o \quad (\varepsilon_y)_o \quad (\gamma_{xy})_o \quad (\varepsilon_{x,y})_o \quad (\varepsilon_{y,x})_o \quad (\gamma_{xy,xx})_o\}^T$
	Nodal displacement vector	Same as Table 1
	Strain interpolation matrix	$B_s = \begin{bmatrix} 0 & 0 & 0 & 1 & 0 & 0 & y & 0 & 0 \\ 0 & 0 & 0 & 0 & 1 & 0 & 0 & x & 0 \\ 0 & 0 & 0 & 0 & 0 & 1 & 0 & 0 & x^2 + y^2 \end{bmatrix}$
	Displacement interpolation matrix	$N_s = \begin{bmatrix} 1 & 0 & -y & x & 0 & \frac{y}{2} & xy & -\frac{y^2}{2} & \frac{y^3}{3} \\ 0 & 1 & x & 0 & y & \frac{x}{2} & -\frac{x^2}{2} & xy & \frac{x^3}{3} \\ 0 & 0 & 1 & 0 & 0 & 0 & -x & y & \frac{x^2 - y^2}{2} \end{bmatrix}$
	Geometric matrix	Same as Table 1

previously reviewed finite elements (see Table 6). Here, the first sub-matrices are derived by replacing the node coordinates in the matrix N_s while for the last two sub-matrices, a different relation was utilized (see Table 6).

Despite its irregular degrees of freedom, the numerical evaluations showed that the performance of this element is better than many of the previous membrane elements. There are different reasons for the better performance of this element. First, all the components of its strain field had the complete term for a linear approximation. Moreover, the equilibrium equations are imposed on the assumed strain field, and the independent strain states are excluded from the strain state vector. The later property provides also the advantage of reducing the number of degrees of freedom in the element. These investigators realized that the geometry of the element and its node locations also had significant effects on its performance. This influence resulted in a new series of more accurate elements, which will be discussed in the coming sections [58, 59, 61, 62].

Table 6: Details of the first triangular element proposed by Rezaiee-Pajand and Yaghoobi [65]

Ref	Properties	Geometry
Rezaiee-Pajand and Yaghoobi [65]	Geometry	
	Strain field	$\begin{cases} \varepsilon_x(x, y) = (\varepsilon_x)_o + (\varepsilon_{x,x})_o x + (\varepsilon_{x,y})_o y \\ \varepsilon_y(x, y) = (\varepsilon_y)_o + (\varepsilon_{y,x})_o x + (\varepsilon_{y,y})_o y \\ \gamma_{xy}(x, y) = (\gamma_{xy})_o + (\gamma_{xy,x})_o x + (\gamma_{xy,y})_o y \end{cases}$
	Strain state vector	$S = \{u_o \quad v_o \quad r_o \quad (\varepsilon_x)_o \quad (\varepsilon_y)_o \quad (\gamma_{xy})_o \quad (\varepsilon_{x,x})_o \quad (\varepsilon_{x,y})_o \quad (\varepsilon_{y,x})_o \quad (\varepsilon_{y,y})_o\}^T$
	Nodal displacement vector	$D = \{D_{2i-1} \quad D_{2i} \quad D_{2j-1} \quad D_{2j} \quad D_{2k-1} \quad D_{2k} \quad D_{2l-1} \quad D_{2l} \quad D_m \quad D_n\}^T$
	Strain interpolation matrix	$B_s = \begin{bmatrix} 0 & 0 & 0 & 1 & 0 & 0 & x & y & 0 & 0 \\ 0 & 0 & 0 & 0 & 1 & 0 & 0 & 0 & x & y \\ 0 & 0 & 0 & 0 & 0 & 1 & -\frac{(2G+\lambda)y}{G} & -\frac{\lambda}{G}x & -\frac{\lambda}{G}y & -\frac{(2G+\lambda)x}{G} \end{bmatrix}$
	Displacement interpolation matrix	$N_s = \begin{bmatrix} 1 & 0 & -y & x & 0 & \frac{y}{2} & \frac{x^2}{2} & -\frac{(2G+\lambda)y^2}{2G} & xy & -y^2 \left(\frac{\lambda}{2G} + \frac{1}{2}\right) & 0 \\ 0 & 1 & x & 0 & y & \frac{x}{2} & 0 & 0 & -x^2 \left(\frac{\lambda}{2G} + \frac{1}{2}\right) & xy & \frac{y^2}{2} - \frac{(2G+\lambda)x^2}{2G} \end{bmatrix}$
	Geometric matrix	$A = [N_{si} \quad N_{sj} \quad N_{sk} \quad N_{sl} \quad N_{sm} \quad N_{sn}]^T$ $N_{s\beta} = \begin{bmatrix} \sin(\alpha) & \cos(\alpha) & x_\beta \cos(\alpha) - y_\beta \sin(\alpha) \\ x_\beta \sin(\alpha) & y_\beta \cos(\alpha) & \frac{x_\beta \cos(\alpha)}{2} - \frac{y_\beta \sin(\alpha)}{2} \\ \left(\frac{x_\beta^2}{2} - \frac{(2G+\lambda)y_\beta^2}{2G}\right) \sin(\alpha) \\ (x_\beta y_\beta) \sin(\alpha) - \left(x_\beta^2 \left(\frac{\lambda}{2G} + \frac{1}{2}\right)\right) \cos(\alpha) \\ (x_\beta y_\beta) \cos(\alpha) - \left(y_\beta^2 \left(\frac{\lambda}{2G} + \frac{1}{2}\right)\right) \sin(\alpha) \\ \left(\frac{y_\beta^2}{2} - \frac{(2G+\lambda)x_\beta^2}{2G}\right) \cos(\alpha) \end{bmatrix} \quad \beta = m, n$

4.7 Rezaiee-Pajand and Yaghoobi (2014- second triangular element)

In another study, Rezaiee-Pajand and Yaghoobi [66] utilized the complete linear strain field of the previous study, but with a different element geometry. In this work, they proposed a seven-node triangular element, which is depicted in Table 7. Six of the ten required degrees of freedom were allocated at the vertex nodes, which had two translational degrees of freedom each. Three mid-side nodes had only one translational degrees of freedom perpendicular to their sides, and the last degree of freedom was a drilling one at the center node. The first three sub-matrices for nodes i , j , and k of the geometric matrix, A , are derived by replacing the coordinates of these nodes in the displacement interpolation matrix. For the three mid-side nodes, the respective sub-matrix is computed by using the equation given in Table 6 for $N_{s\beta}$. Finally, the last sub-matrix, N_{so} , is derived from the next equality presented in the last row of Table 7, after the geometric matrix. The authors developed this formulation for geometrical nonlinear analysis of plane structures. For this purpose, they took advantage of the co-rotational formulation [54, 3]. For this purpose, a local coordinate system, which its origin was located at the center of the element, was considered. This coordinate system translates and rotates with the element. Then, the element was formulated in this new system. Since the nonlinear analysis was not in the scope of this study, for further information about the co-rotational formulation, one can refer to references [54, 66].

4.8 Rebiai (2018)

In a more recent attempt to propose three-node nine-degree of freedom triangular element, Rebiai [48] suggested a new strain-based element with incomplete second-order strain field. This strain field satisfies the compatibility condition, but the equilibrium conditions were not fulfilled within the element. In fact, Rebiai did not intend to impose the equilibrium equations, (Please see Table 8).

4.9 Rezaiee-Pajand, Gharaei-Moghaddam, and Ramezani (2019- first triangular element)

In one of the most-recent studies, Rezaiee-Pajand, Gharaei-Moghaddam, and Ramezani [58] suggested new triangular elements. They utilized the complete linear strain field, which was the same as the previous studies by Rezaiee-

Table 7: Details of the second triangular element proposed by Rezaiee-Pajand and Yaghoobi [66]

Ref	Properties	Geometry
Rezaiee-Pajand and Yaghoobi [66]	Geometry	
	Strain field	Same as Table 6
	Strain state vector	Same as Table 6
	Nodal displacement vector	$D = \{D_{2i-1} \ D_{2i} \ D_{2j-1} \ D_{2j} \ D_{2k-1} \ D_{2k} \ D_l \ D_m \ D_n \ D_p\}^T$
	Strain interpolation matrix	Same as Table 6
	Displacement interpolation matrix	Same as Table 6
	Geometric matrix	$A = [N_{si} \ N_{sj} \ N_{sk} \ N_{sl} \ N_{sm} \ N_{sn} \ N_{sp}]^T$ $N_{sp} = \begin{bmatrix} 0 & 0 & 1 & 0 & 0 & 0 & \frac{(2G+\lambda)y_p}{2G} \\ -\frac{(2G+\lambda)x_p}{2G} & \frac{(2G+\lambda)y_p}{2G} & -\frac{(2G+\lambda)x_p}{2G} \end{bmatrix}$

Pajand and Yaghoobi [65, 66]. Moreover, they also imposed the equilibrium condition to specify the dependent strain states. The differences between these new elements and previous ones are in the geometry of the elements. In their first element, the authors assumed a five-node triangular element, with three vertex and two mid-side nodes (see Table 9). Each node has two translational degrees of freedom.

As mentioned previously, it has been proved through extensive investigations, that configuration of the nodes and distribution of the degrees of freedom have been influential in the performance of the resulting elements [65, 66]. Numerical studies showed that the last presented element provided

Table 8: Details of the triangular element proposed by Rebiai [48]

Ref	Properties	Geometry
Rebiai [48]	Geometry	Same as Table 1
	Strain field	$\begin{cases} \varepsilon_x(x, y) = (\varepsilon_x)_o + (\varepsilon_{x,y})_o y + (\varepsilon_{x,yy})_o y^2 \\ \varepsilon_y(x, y) = (\varepsilon_y)_o + (\varepsilon_{y,x})_o x + (\varepsilon_{x,yy})_o x^2 \\ \gamma_{xy}(x, y) = (\gamma_{xy})_o + 2(\varepsilon_{x,yy})_o x^2 + 2(\varepsilon_{x,yy})_o y^2 + 4(\varepsilon_{x,yy})_o xy \end{cases}$
	Strain state vector	$S = \{u_o \quad v_o \quad r_o \quad (\varepsilon_x)_o \quad (\varepsilon_y)_o \quad (\gamma_{xy})_o \quad (\varepsilon_{x,y})_o \quad (\varepsilon_{y,x})_o \quad (\varepsilon_{x,yy})_o\}^T$
	Nodal displacement vector	Same as Table 1
	Strain interpolation matrix	$B_s = \begin{bmatrix} 0 & 0 & 0 & 1 & 0 & 0 & y & 0 & y^2 \\ 0 & 0 & 0 & 0 & 1 & 0 & 0 & x & x^2 \\ 0 & 0 & 0 & 0 & 0 & 1 & 0 & 0 & 2(x+y)^2 \end{bmatrix}$
	Displacement interpolation matrix	$N_s = \begin{bmatrix} 1 & 0 & -y & x & 0 & \frac{y}{2} & xy & -\frac{y^2}{2} & \frac{2y^3}{3} + xy^2 \\ 0 & 1 & x & 0 & y & \frac{x}{2} & -\frac{x^2}{2} & xy & \frac{2x^3}{3} + yx^2 \\ 0 & 0 & 1 & 0 & 0 & 0 & -x & y & x^2 - y^2 \end{bmatrix}$
	Geometric matrix	Same as Table 1

very accurate responses, especially for the elements under the bending loads. Something that might be questionable about the geometry of this element was the arbitrariness in the selection of the sides with mid nodes. To show that this selection did not have considerable effect on the performance of the element, the authors solved a numerical example with different locations of the mid-side nodes, and the results were identical. Moreover, the main idea behind this selection was to produce a powerful finite element for transitional purposes. To demonstrate this fact, Rezaiee-Pajand, Gharaei-Moghaddam, and Ramezani [58] investigated the performance of this element as a transitional element in numerical example and compared its behavior with standard displacement-based transitional elements. The results showed superiority of the mentioned element.

4.10 Rezaiee-Pajand, Gharaei-Moghaddam, and Ramezani (2019- second triangular element)

After presenting the previous element, Rezaiee-Pajand, Gharaei-Moghaddam, and Ramezani [58] considered another configuration for the complete linear strain field. In this element, the authors considered the well-known three node nine-degree of freedom triangular element and added an internal node with one translational degree of freedom in an arbitrary direction. This element geometry is demonstrated in Table 10. By using (33), the displacement of the

Table 9: Details of the first triangular element proposed by Rezaiee-Pajand, Gharaei-Moghaddam, and Ramezani [58]

Ref	Properties	Geometry
Rezaiee-Pajand and Gharaei-Moghaddam [58]	Geometry	
	Strain field	Same as Table 6
	Strain state vector	Same as Table 6
	Nodal displacement vector	$D = \{D_{2i-1} \ D_{2i} \ D_{2j-1} \ D_{2j} \ D_{2k-1} \ D_{2k} \ D_{2l-1} \ D_{2l} \ D_{2m-1} \ D_{2m}\}^T$
	Strain interpolation matrix	$B_s = \begin{bmatrix} 0 & 0 & 0 & 1 & 0 & 0 & x & y & 0 & 0 \\ 0 & 0 & 0 & 0 & 1 & 0 & 0 & 0 & x & y \\ 0 & 0 & 0 & 0 & 0 & 1 & -\frac{(2G+\lambda)y}{G} & -\frac{\lambda}{G}x - \frac{\lambda}{G}y & -\frac{(2G+\lambda)x}{G} \end{bmatrix}$
	Displacement interpolation matrix	$N_s = \begin{bmatrix} 1 & 0 & -y & x & 0 & \frac{y}{2} & \frac{x^2}{2} - \frac{(2G+\lambda)y^2}{2G} & xy & -y^2(\frac{\lambda}{2G} + \frac{1}{2}) & 0 \\ 0 & 1 & x & 0 & y & \frac{x}{2} & 0 & -x^2(\frac{\lambda}{2G} + \frac{1}{2}) & xy & \frac{y^2}{2} - \frac{(2G+\lambda)x^2}{2G} \end{bmatrix}$
	Geometric matrix	$A = [N_{si} \ N_{sj} \ N_{sk} \ N_{sl} \ N_{sm}]^T$

internal node can be connected to the displacements in x and y directions. The internal node of the element can be removed by the static condensation approach, and therefore, the element becomes a three-node nine-degrees of freedom triangular element, which is a common element in general finite element programs. This element provided surprisingly accurate results under different types of loading and especially shear loading, in which many of the available elements failed to provide the exact response in the case of distorted mesh [58]. In addition to the fast convergence and high accuracy, this element was highly insensitive to the mesh distortion. Numerical examinations demonstrated that the direction of internal degree of freedom did not have any noticeable effect on the accuracy and performance of the element [58].

Table 10: Details of the second triangular element proposed by Rezaiee-Pajand, Gharaei-Moghaddam, and Ramezani [58]

Ref	Properties	Geometry
Rezaiee-Pajand and Gharaei-Moghaddam [58]	Geometry	
	Strain field	Same as Table 6
	Strain state vector	Same as Table 6
	Nodal displacement vector	$D = \{D_{2i-1} \ D_{2i} \ D_{2j-1} \ D_{2j} \ D_{2k-1} \ D_{2k} \ D_{2l-1} \ D_{2l}\ D_{2m-1} \ D_{2m}\}^T$
	Strain interpolation matrix	$B_s = \begin{bmatrix} 0 & 0 & 0 & 1 & 0 & 0 & x & y & 0 & 0 \\ 0 & 0 & 0 & 0 & 1 & 0 & 0 & 0 & x & y \\ 0 & 0 & 0 & 0 & 0 & 1 & -\frac{(2G+\lambda)y}{G} & -\frac{\lambda}{G}x & -\frac{\lambda}{G}y & -\frac{(2G+\lambda)x}{G} \end{bmatrix}$
	Displacement interpolation matrix	$N_{s\beta} = \begin{bmatrix} 1 & 0 & -y_\beta & x_\beta & 0 & \frac{y_\beta}{2} & \frac{x_\beta^2}{2} - \frac{(2G+\lambda)y_\beta^2}{2G} & x_\beta y_\beta & -y_\beta^2 \left(\frac{\lambda}{2G} + \frac{1}{2}\right) & 0 \\ 0 & 1 & x_\beta & 0 & y_\beta & \frac{x_\beta}{2} & 0 & -x_\beta^2 \left(\frac{\lambda}{2G} + \frac{1}{2}\right) & x_\beta y_\beta & \frac{x_\beta^2}{2} - \frac{(2G+\lambda)y_\beta^2}{2G} \\ 0 & 0 & 1 & 0 & 0 & 0 & \frac{(2G+\lambda)y_\beta}{2G} & -\frac{(2G+\lambda)x_\beta}{2G} & \frac{(2G+\lambda)y_\beta}{2G} & -\frac{(2G+\lambda)x_\beta}{2G} \end{bmatrix}$ $\beta = i, j, k$
Geometric matrix	$A = [N_{si} \ N_{sj} \ N_{sk} \ N_{sl}]^T$ $N_{sl} = \begin{bmatrix} \sin(\alpha) & \cos(\alpha) & x_l \cos(\alpha) - y_l \sin(\alpha) & x_l \sin(\alpha) & y_l \cos(\alpha) \\ \frac{x_l \cos(\alpha)}{2} - \frac{y_l \sin(\alpha)}{2} & \left(\frac{x_l^2}{2} - \frac{(2G+\lambda)y_l^2}{2G}\right) \sin(\alpha) \\ (x_l y_l) \sin(\alpha) - \left(x_l^2 \left(\frac{\lambda}{2G} + \frac{1}{2}\right)\right) \cos(\alpha) \\ (x_l y_l) \cos(\alpha) - \left(y_l^2 \left(\frac{\lambda}{2G} + \frac{1}{2}\right)\right) \sin(\alpha) \\ \left(\frac{y_l^2}{2} - \frac{(2G+\lambda)x_l^2}{2G}\right) \cos(\alpha) \end{bmatrix}$	

4.11 Rezaiee-Pajand, Gharaei-Moghaddam, and Ramezani (2019- third triangular element)

In another study, Rezaiee-Pajand, Gharaei-Moghaddam, and Ramezani [59] formulated a higher-order strain-based assuming complete second-order normal strains and linear shear strains (see Table 11). After imposing the equilibrium and compatibility conditions on the assumed strain field, seven de-

pendent strain states were excluded and eleven independent strain states remained.

Table 11: Details of the third triangular element proposed by Rezaiee-Pajand, Gharaei-Moghaddam, and Ramezani [59]

Ref	Properties	Geometry
Rezaiee-Pajand et al. [59]	Geometry	
	Strain field	$\begin{cases} \varepsilon_x(x, y) = (\varepsilon_x)_o + (\varepsilon_{x,x})_o x + (\varepsilon_{x,y})_o y + (\varepsilon_{x,xx})_o \left(\frac{x^2}{2}\right) \\ \quad + (\varepsilon_{x,xy})_o (xy) + (\varepsilon_{x,yy})_o \left(\frac{y^2}{2}\right) \\ \varepsilon_y(x, y) = (\varepsilon_y)_o + (\varepsilon_{y,x})_o x + (\varepsilon_{y,y})_o y + (\varepsilon_{y,xx})_o \left(\frac{x^2}{2}\right) \\ \quad + (\varepsilon_{y,xy})_o (xy) + (\varepsilon_{y,yy})_o \left(\frac{y^2}{2}\right) \\ \gamma_{xy}(x, y) = (\gamma_{xy})_o + (\gamma_{xy,x})_o x + (\gamma_{xy,y})_o y \end{cases}$
	Strain state vector	$S = \{u_o \quad v_o \quad r_o \quad (\varepsilon_x)_o \quad (\varepsilon_y)_o \quad (\gamma_{xy})_o \quad (\varepsilon_{x,x})_o \quad (\varepsilon_{x,y})_o \quad (\varepsilon_{y,x})_o \quad (\varepsilon_{y,y})_o \quad (\varepsilon_{x,yy})_o\}^T$
	Nodal displacement vector	$D = \{D_{2i-1} \quad D_{2i} \quad D_{2j-1} \quad D_{2j} \quad D_{2k-1} \quad D_{2k} \quad D_l \quad D_m \quad D_n \quad D_{2p-1} \quad D_{2p}\}^T$
	Strain interpolation matrix	$B_s = \begin{bmatrix} 0 & 0 & 0 & 1 & 0 & 0 & x & y & 0 & 0 & \frac{y^2}{2} + \frac{\lambda x^2}{2(2G+\lambda)} \\ 0 & 0 & 0 & 0 & 1 & 0 & 0 & 0 & x & y & -\frac{x^2}{2} + \frac{\lambda y^2}{2(2G+\lambda)} \\ 0 & 0 & 0 & 0 & 0 & 1 & -\frac{(2G+\lambda)y}{G} & -\frac{\lambda}{G}x & -\frac{\lambda}{G}y & -\frac{(2G+\lambda)x}{G} & 0 \end{bmatrix}$
	Displacement interpolation matrix	$N_s = \begin{bmatrix} 1 & 0 & -y & x & 0 & \frac{y}{2} & \frac{x^2}{2} & -\frac{(2G+\lambda)y^2}{2G} & xy & -y^2 \frac{(G+\lambda)}{2G} & 0 & -\frac{x^3}{6} \frac{\lambda}{(2G+\lambda)} + \frac{xy^2}{2} \\ 0 & 1 & x & 0 & y & \frac{x}{2} & 0 & 0 & -x^2 \frac{(G+\lambda)}{2G} & xy & \frac{y^2}{2} - \frac{(2G+\lambda)x^2}{2G} & -\frac{y^3}{6} \frac{\lambda}{(2G+\lambda)} + \frac{yx^2}{2} \end{bmatrix}$
	Geometric matrix	$A = [N_{si} \quad N_{sj} \quad N_{sk} \quad T_{sl} \quad T_{sm} \quad T_{sn} \quad N_{so}]^T$ $T_s = \begin{bmatrix} 0 & 0 & 1 & 0 & 0 & 0 & \frac{(2G+\lambda)y}{2G} & -\frac{(2G+\lambda)x}{2G} & \frac{(2G+\lambda)y}{2G} & -\frac{(2G+\lambda)x}{2G} & -xy \end{bmatrix}$

The selected geometry of the element is demonstrated in Table 11. As it can be seen, the element had seven nodes and eleven degrees of freedom in agreement with the independent strain states.

4.12 Rezaiee-Pajand, Gharaei-Moghaddam, and Ramezani (2020- fourth triangular element)

Rezaiee-Pajand, Gharaei-Moghaddam, and Ramezani [61] utilized the assumed strain of their previous study [59] to formulate another higher-order strain-based element. The difference of this element with the previous one is the geometry of the element, which is demonstrated in Table 12.

Table 12: Details of the fourth triangular element proposed by Rezaiee-Pajand, Gharaei-Moghaddam, and Ramezani [61]

Ref	Properties	
Rezaiee-Pajand et al. [61]	Geometry	<p>The diagram shows a triangular element with nodes i, j, and k. Node i is at the bottom-left, node j is at the bottom-right, and node k is at the top. A Cartesian coordinate system (X, Y) is shown with the origin at node i. At each node, there are two displacement degrees of freedom: D_{3i-1} (vertical) and D_{3i-2} (horizontal) at node i; D_{3j-1} (vertical) and D_{3j-2} (horizontal) at node j; and D_{3k-1} (vertical) and D_{3k-2} (horizontal) at node k. Additionally, there is a central node l with two displacement degrees of freedom: D_{2l} (vertical) and D_{2l-1} (horizontal).</p>
	Strain field	Same as Table 11
	Strain state vector	Same as Table 11
	Nodal displacement vector	$D = \{D_{3i-2} \ D_{3i-1} \ D_{3i} \ D_{3j-2} \ D_{3j-1} \ D_{3j} \ D_{3k-2} \ D_{3k-1} \ D_{3k} \ D_{2l-1} \ D_{2l}\}^T$
	Strain interpolation matrix	Same as Table 11
	Displacement interpolation matrix	Same as Table 11
	Geometric matrix	$A_G = [N_{si} \ T_{si} \ N_{sj} \ T_{sj} \ N_{sk} \ T_{sl} \ N_{sl} \ N_{sm} \ N_{sn} \ N_{so}]^T$

4.13 Rezaiee-Pajand, Ramezani, and Gharaei-Moghaddam (2020- fifth triangular element)

Since it was expected that using higher-order strain fields improves the accuracy of the elements, Rezaiee-Pajand, Ramezani, and Gharaei-Moghaddam [62] formulated a seven-node triangular element using complete second-order strain field (see Table 13). In this element formulation, the compatibility and equilibrium conditions were again satisfied.

Table 13: Details of the fifth triangular element proposed by Rezaiee-Pajand, Ramezani, and Gharaei-Moghaddam [62]

Ref	Properties	
Rezaiee-Pajand et al. [62]	Geometry	
	Strain field	$\begin{cases} \varepsilon_x(x, y) = (\varepsilon_x)_o + (\varepsilon_{x,x})_o x + (\varepsilon_{x,y})_o y + (\varepsilon_{x,xx})_o \left(\frac{x^2}{2}\right) \\ \quad + (\varepsilon_{x,xy})_o (xy) + (\varepsilon_{x,yy})_o \left(\frac{y^2}{2}\right) \\ \varepsilon_y(x, y) = (\varepsilon_y)_o + (\varepsilon_{y,x})_o x + (\varepsilon_{y,y})_o y + (\varepsilon_{y,xx})_o \left(\frac{x^2}{2}\right) \\ \quad + (\varepsilon_{y,xy})_o (xy) + (\varepsilon_{y,yy})_o \left(\frac{y^2}{2}\right) \\ \gamma_{xy}(x, y) = (\gamma_{xy})_o + (\gamma_{xy,x})_o x + (\gamma_{xy,y})_o y + (\gamma_{xy,xx})_o \left(\frac{x^2}{2}\right) \\ \quad + (\gamma_{xy,xy})_o (xy) + (\gamma_{xy,yy})_o \left(\frac{y^2}{2}\right) \end{cases}$
	Nodal displacement vector	$D = \{D_{2i-1} \ D_{2i} \ D_{2j-1} \ D_{2j} \ D_{2k-1} \ D_{2k} \ D_{2l-1} \ D_{2l} \ D_{2m-1} \ D_{2m} \ D_{2n-1} \ D_{2n} \ D_{2o-1} \ D_{2o}\}^T$
	Strain interpolation matrix	$B_s = \begin{bmatrix} 0 & 0 & 0 & 1 & 0 & 0 & x & y & 0 & 0 & \frac{y^2}{2} - \frac{(G+\lambda)^2 x^2}{2G} - \frac{\lambda x^2}{2G} & xy & -\frac{(G+\lambda)x^2}{2K} & 0 \\ 0 & 0 & 0 & 0 & 1 & 0 & 0 & 0 & x & y & -\frac{(G+\lambda)y^2}{2G} & 0 & \frac{x^2}{2} - \frac{Gy^2}{2K} & xy \\ 0 & 0 & 0 & 0 & 0 & 1 & -\frac{Ky}{G} - \frac{\lambda}{G}x - \frac{\lambda}{G}y - \frac{Kx}{G} & xy & -\frac{Ky^2}{2G} - \frac{\lambda x^2}{2G} & xy & -\frac{Kx^2}{2G} - \frac{\lambda y^2}{2G} \end{bmatrix}$
	Displacement interpolation matrix	$N_s = \begin{bmatrix} 1 & 0 & -y & x & 0 & \frac{x^2}{2} & \frac{y^2}{2} & -\frac{(2G+\lambda)x^2}{2G} & xy & -y^2 \frac{(G+\lambda)}{2G} & 0 & -\frac{xy^2}{2} - \frac{Gx^3}{2(G+\lambda)} & \frac{xy^2}{2} - \frac{(2G+\lambda)y^2}{6G} & -x^2 \frac{(G+\lambda)}{6G} & -y^3 \frac{(G+\lambda)}{6G} \\ 0 & 1 & x & 0 & y & \frac{x^2}{2} & \frac{y^2}{2} & -x^2 \frac{(G+\lambda)}{2G} & xy & \frac{xy^2}{2} - \frac{(2G+\lambda)x^2}{2G} & -y^2 \frac{(G+\lambda)}{2G} & -y^3 \frac{(G+\lambda)}{6G} & -x^2 \frac{(G+\lambda)}{6G} & \frac{xy^2}{2} - \frac{Gy^3}{6(G+\lambda)} & \frac{(2G+\lambda)x^2}{6G} \end{bmatrix}$
	Geometric matrix	$A_G = [N_{si} \ N_{sj} \ N_{sk} \ N_{sl} \ N_{sm} \ N_{sn} \ N_{so}]^T$

5 Quadrilateral membrane elements

The existing quadrilateral strain-based membrane elements are reviewed in this section. In contrast with the triangular elements, which are mostly developed by the assumption of linear or second-order strain-field, higher-order strain fields were utilized in the formulation of quadrilateral elements. In the quadrilateral elements, there are two common configurations. The first one is a four-node twelve-degrees of freedom quadrilateral element, and the second common geometry is a five-node ten-degrees of freedom element. More details are provided in the following.

5.1 Sabir and Sfindji (1995)

Like the triangular elements, the first quadrilateral element is proposed by Sabir [72]. In 1995, Sabir and Sfindji suggested a rectangular strain-based finite element with linear strain field.

Once again, they assumed strain components satisfy compatibility condition, but the equilibrium equations are not fulfilled. Due to the existence of ten strain states, ten degrees of freedom are required. Therefore, Sabir and Sfindji considered the five-node rectangular element depicted in Table 15. Each node of this element has two translational degrees of freedom.

5.2 Tayeh (2003)

Another rectangular element was proposed by Tayeh [75]. He utilized an incomplete fourth-order approximation for normal strains and incomplete second-order assumption for the shear strain (see Table 15).

In agreement with these twelve strain states, a four-node rectangular element with three degrees of freedom at each node was considered. It should be noted that this element and the previous one proposed by Sabir and Sfindji had rectangular geometry, according to the original articles [72, 75], but based on the basics of strain- formulation, the effect of the geometry only entered in geometric matrix, A . So, by using the nodes of a general quadrilateral shape in construction of this matrix; the mentioned elements can have a general quadrilateral geometry.

Table 14: Details of the Rectangular element proposed by Sabir and Sfindji [72]

Ref	Properties	
Sabir and Sfindji [72]	Geometry	
	Strain field	Same as Table 2
	Strain state vector	$S = \{u_o \quad v_o \quad r_o \quad (\varepsilon_x)_o \quad (\varepsilon_y)_o \quad (\gamma_{xy})_o \quad (\varepsilon_{x,y})_o \quad (\varepsilon_{y,x})_o \quad (\gamma_{xy,x})_o \quad (\gamma_{xy,y})_o\}^T$
	Nodal displacement vector	$D = \{D_{2i-1} \quad D_{2i} \quad D_{2j-1} \quad D_{2j} \quad D_{2k-1} \quad D_{2k} \quad D_{2l-1} \quad D_{2l} \quad D_{2m-1} \quad D_{2m}\}^T$
	Strain interpolation matrix	$B_s = \begin{bmatrix} 0 & 0 & 0 & 1 & 0 & 0 & y & 0 & 0 & 0 \\ 0 & 0 & 0 & 0 & 1 & 0 & 0 & x & 0 & 0 \\ 0 & 0 & 0 & 0 & 0 & 1 & 0 & 0 & x & y \end{bmatrix}$
	Displacement interpolation matrix	$N_s = \begin{bmatrix} 1 & 0 & -y & x & 0 & \frac{y}{2} & xy & \frac{-y^2}{2} & 0 & \frac{y^2}{2} \\ 0 & 1 & x & 0 & y & \frac{x}{2} & -\frac{x^2}{2} & xy & \frac{xyx^2}{2} & 0 \end{bmatrix}$
	Geometric matrix	$A = [N_{si} \quad N_{sj} \quad N_{sk} \quad N_{sl} \quad N_{sm}]^T$

5.3 Belarbi and Maalem (2005)

In 2005, Belarbi and Maalem [12] suggested an improved strain-based rectangular element by the assumption of linear normal strains and constant shear strain. The element geometry and distribution of nodes and degrees of freedom are the one proposed by Sabir and Sfindji.

Table 15: Details of the Rectangular element proposed by Tayeh [75]

Ref	Properties	
Tayeh [75]	Geometry	
	Strain field	$\begin{cases} \varepsilon_x(x, y) = (\varepsilon_x)_o + (\varepsilon_{x,y})_o y + (\varepsilon_{x,yy})_o y^2 + (\varepsilon_{x,yyy})_o xy^3 \\ \varepsilon_y(x, y) = (\varepsilon_y)_o + (\varepsilon_{y,x})_o x - (\varepsilon_{x,yy})_o x^2 - (\varepsilon_{x,yyy})_o yx^3 \\ \gamma_{xy}(x, y) = (\gamma_{xy})_o + (\gamma_{xy,x})_o x + (\gamma_{xy,y})_o y - (\varepsilon_{x,y})_o \frac{x^2}{2} - (\varepsilon_{y,x})_o \frac{y^2}{2} \end{cases}$
	Strain state vector	$S = \{u_o \quad v_o \quad r_o \quad (\varepsilon_x)_o \quad (\varepsilon_y)_o \quad (\gamma_{xy})_o \quad (\varepsilon_{x,y})_o \quad (\varepsilon_{y,x})_o \quad (AE_{xy,x})_o \quad (\gamma_{xy,y})_o \quad (\varepsilon_{x,yy})_o \quad (\varepsilon_{x,yyy})_o\}^T$
	Nodal displacement vector	$D = \{D_{3i-2} \quad D_{3i-1} \quad D_{3j-2} \quad D_{3j-1} \quad D_{3k-2} \quad D_{3k-1} \quad D_{3l-2} \quad D_{3l-1}\}^T$
	Strain interpolation matrix	$B_s = \begin{bmatrix} 0 & 0 & 0 & 1 & 0 & 0 & y & 0 & 0 & 0 & y^2 & xy^3 \\ 0 & 0 & 0 & 0 & 1 & 0 & 0 & x & 0 & 0 & -x^2 & -x^3 y \\ 0 & 0 & 0 & 0 & 0 & 1 & -\frac{x^2}{2} & -\frac{y^2}{2} & x & y & 0 & 0 \end{bmatrix}$
	Displacement interpolation matrix	$N_s = \begin{bmatrix} 1 & 0 & -y & x & 0 & \frac{y}{2} & xy & -\frac{y^3}{6} - \frac{y^2}{2} & 0 & \frac{y^2}{2} & xy^2 & \frac{x^2 y^3}{2} \\ 0 & 1 & x & 0 & y & \frac{x}{2} & -\frac{x^3}{6} - \frac{x^2}{2} & xy & \frac{x^2}{2} & 0 & -x^2 y & -\frac{x^3 y^2}{2} \\ 0 & 0 & 1 & 0 & 0 & 0 & -\frac{x^2}{4} - x & \frac{y^2}{4} + y & \frac{x}{2} & -\frac{y}{2} & -2xy & -\frac{3x^2 y^2}{2} \end{bmatrix}$
	Geometric matrix	$A = [N_{si} \quad N_{sj} \quad N_{sk} \quad N_{sl}]^T$

5.4 Rezaiee-Pajand and Yaghoobi (2012- first quadrilateral element)

The first strain-based generalized quadrilateral plane element, which its strain field satisfies both compatibility and equilibrium conditions, is proposed by Rezaiee-Pajand and Yaghoobi [63]. They [65, 66] took advantage of the linear strain field that they had used for development of triangular elements (see Table 6). After imposing the equilibrium criteria and determination of dependent strain states, ten independent strain states remain for the re-

Table 16: Details of the Rectangular element proposed by Belarbi and Maalem [12]

Ref	Properties	
Belarbi and Maalem [12]	Geometry	Same as Table 14
	Strain field	$\begin{cases} \varepsilon_x(x, y) = (\varepsilon_x)_o + (\varepsilon_{x,y})_o y + (\varepsilon_{x,x})_o x \\ \varepsilon_y(x, y) = (\varepsilon_y)_o + (\varepsilon_{y,x})_o x + (\varepsilon_{y,y})_o y \\ \gamma_{xy}(x, y) = (\gamma_{xy})_o \end{cases}$
	Strain state vector	$S = \{u_o \quad v_o \quad r_o \quad (\varepsilon_x)_o \quad (\varepsilon_y)_o \quad (\gamma_{xy})_o \quad (\varepsilon_{x,y})_o \quad (\varepsilon_{x,x})_o \quad (\varepsilon_{y,x})_o \quad (\varepsilon_{y,y})_o\}^T$
	Nodal displacement vector	Same as Table 14
	Strain interpolation matrix	$B_s = \begin{bmatrix} 0 & 0 & 0 & 1 & 0 & 0 & y & x & 0 & 0 \\ 0 & 0 & 0 & 0 & 1 & 0 & 0 & 0 & x & y \\ 0 & 0 & 0 & 0 & 0 & 1 & 0 & 0 & 0 & 0 \end{bmatrix}$
	Displacement interpolation matrix	$N_s = \begin{bmatrix} 1 & 0 & -y & x & 0 & \frac{y}{2} & xy & \frac{x^2}{2} & -\frac{y^2}{2} & 0 \\ 0 & 1 & x & 0 & y & \frac{x}{2} & -\frac{x^2}{2} & 0 & xy & \frac{y^2}{2} \end{bmatrix}$
	Geometric matrix	Same as Table 14

quired ten degrees of freedom. Rezaiee-Pajand and Yaghoobi considered the generalized five-node quadrilateral element, which is depicted in Table 17.

In another study, Rezaiee-Pajand and Yaghoobi [64] investigated the performance of two special rectangular variants of the generalized quadrilateral element. In the first element, the fifth node was located in its center, while this node was moved to the middle of one side in the next element. In this study, they showed that these strain-based elements were less sensitive to mesh distortion in comparison with their displacement-based counterparts. Moreover, they displayed that strain-based elements were completely free from shear parasitic errors.

5.5 Rebiai and Belounar (2013- first quadrilateral element)

A four-node rectangular strain-based element with incomplete fourth-order normal strains was proposed by Rebiai and Belounar [49]. The authors assumed linear shear strains for this element. This strain field, had twelve independent strain states. Regarding this field, it seems that there was no clear and rational basis behind this selection. Therefore, this field was probably the result of the trial-and-error process to attain the best performance of the resulting element. Rebiai and Belounar developed this element for axisymmetric, as well as, elastoplastic analysis of structures. For the nonlinear

Table 17: Details of the first quadrilateral element proposed by Rezaiee-Pajand and Yaghoobi [63]

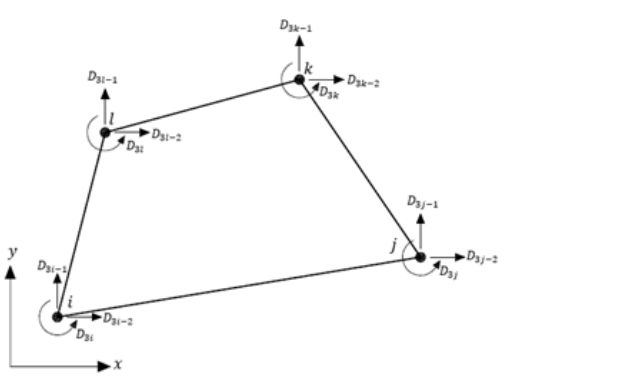
Ref	Properties	Geometry
Rezaiee-Pajand and Yaghoobi [63]	Geometry	
	Strain field	Same as Table 6
	Strain state vector	Same as Table 6
	Nodal displacement vector	$D = \{D_{2i-1} \ D_{2i} \ D_{2j-1} \ D_{2j} \ D_{2k-1} \ D_{2k} \ D_{2l-1} \ D_{2l} \ D_{2m-1} \ D_{2m}\}^T$
	Strain interpolation matrix	Same as Table 6
	Displacement interpolation matrix	Same as Table 6
	Geometric matrix	$A = \{N_{si} \ N_{sj} \ N_{sk} \ N_{sl} \ N_{sm}\}^T$

analysis, they took advantage of the Mohr–Coulomb yield criteria and the initial stress and strain methods [49]. They showed that the strain-based elements provided reliable and accurate results in nonlinear problems.

5.6 Rebiai and Belouar (2014- second quadrilateral element)

In another research work, Rebiai and Belouar suggested another variant of their previous element [50]. In this new element, they considered the strain field of their previous study [50], but added new linear term to the shear strain and changed the dependent term of the normal strains.

Table 18: Details of the first quadrilateral element proposed by Rebiai and Beloumar [49]

Ref	Properties	
Rebiai and Beloumar [49]	Geometry	
	Strain field	$\begin{cases} \varepsilon_x(x, y) = (\varepsilon_x)_o + (\varepsilon_{x,y})_o y + (\varepsilon_{x,x})_o x + (\varepsilon_{x,yy})_o y^2 + 2(\varepsilon_{x,xyyy})_o xy^3 \\ \varepsilon_y(x, y) = (\varepsilon_y)_o + (\varepsilon_{x,x})_o x + 2(\varepsilon_{y,y})_o y - (\varepsilon_{x,yy})_o x^2 - 2(\varepsilon_{x,xyyy})_o yx^3 \\ \gamma_{xy}(x, y) = 2(\gamma_{xy})_o + 2(\varepsilon_{x,y})_o x + 2(\varepsilon_{x,x})_o y + 2(\varepsilon_{y,y})_o y + 2(\varepsilon_{x,yy})_o y - 2(\varepsilon_{x,yy})_o x + 2(\gamma_{xy,x})_o x \end{cases}$
	Strain state vector	$S = \{u_o \quad v_o \quad r_o \quad (\varepsilon_x)_o \quad (\varepsilon_y)_o \quad (\gamma_{xy})_o \quad (\varepsilon_{x,y})_o \quad (\varepsilon_{x,x})_o \quad (\varepsilon_{y,y})_o \quad (\gamma_{xy,x})_o \quad (\varepsilon_{x,yy})_o \quad (\varepsilon_{x,xyyy})_o\}^T$
	Nodal displacement vector	$D = \{D_{3i-2} \quad D_{3i-1} \quad D_{3i} \quad D_{3j-2} \quad D_{3j-1} \quad D_{3j} \quad D_{3k-2} \quad D_{3k-1} \quad D_{3k} \quad D_{3l-2} \quad D_{3l-1} \quad D_{3l}\}^T$
	Strain interpolation matrix	$B_s = \begin{bmatrix} 0 & 0 & 0 & 1 & 0 & 0 & y & x & 0 & 0 & y^2 & 2xy^3 \\ 0 & 0 & 0 & 0 & 1 & 0 & 0 & x & 2y & 0 & -x^2 & -2x^3y \\ 0 & 0 & 0 & 0 & 0 & 2 & 2x & 2y & 2y & 2x & 2y - 2x & 0 \end{bmatrix}$
	Displacement interpolation matrix	$N_s = \begin{bmatrix} 1 & 0 & -y & x & 0 & y & xy & \frac{x^2+y^2}{2} & y^2 & 0 & xy^2 + y^2 & x^2y^3 \\ 0 & 1 & x & 0 & y & x & \frac{x^2}{2} & xy & y^2 & x^2 & -x^2y - x^2 & -x^3y^2 \\ 0 & 0 & 1 & 0 & 0 & 0 & 0 & 0 & -y & x & -x - y - 2xy & -3x^2y^2 \end{bmatrix}$
	Geometric matrix	$A = [N_{si} \quad N_{sj} \quad N_{sk} \quad N_{sl}]^T$

Similar to their previous study, Rebiai and Beloumar utilized this element for both linear and materially nonlinear analysis. In their numerical evaluations, they included different yield criteria, such as, Tresca, Von Mises and Mohr-Coulomb. Once more, the attained results demonstrated the superiority of strain formulation in comparison with classical displacement-based elements.

Table 19: Details of the second quadrilateral element proposed by Rebiai and Beloumar [50]

Ref	Properties	
Rebiai and Beloumar [50]	Geometry	Same as Table 18
	Strain field	$\begin{cases} \varepsilon_x(x, y) = (\varepsilon_x)_o + (\varepsilon_{x,y})_o y + (\varepsilon_y)_o x + (\varepsilon_{x,yy})_o y^2 + 2(\varepsilon_{x,xyyy})_o xy^3 \\ \varepsilon_y(x, y) = (\varepsilon_y)_o + (\varepsilon_{y,x})_o x + (\varepsilon_{y,y})_o y - (\varepsilon_{x,yy})_o x^2 - 2(\varepsilon_{x,xyyy})_o xy^3 \\ \gamma_{xy}(x, y) = 2(\gamma_{xy})_o + [2(\gamma_{xy})_o + 2(\varepsilon_{y,x})_o + (\varepsilon_{y,y})_o]y + 2[(\varepsilon_{x,y})_o + (\varepsilon_y)_o + (\gamma_{xy,x})_o]x \end{cases}$
	Strain state vector	$S = \{u_o \quad v_o \quad r_o \quad (\varepsilon_x)_o \quad (\varepsilon_y)_o \quad (\gamma_{xy})_o \quad (\varepsilon_{x,y})_o \quad (\varepsilon_{y,x})_o \quad (\varepsilon_{y,y})_o \quad (\gamma_{xy,x})_o \quad (\varepsilon_{x,yy})_o \quad (\varepsilon_{x,xyyy})_o\}^T$
	Nodal displacement vector	Same as Table 18
	Strain interpolation matrix	$B_s = \begin{bmatrix} 0 & 0 & 0 & 1 & x & 0 & y & 0 & 0 & 0 & y^2 & 2xy^3 \\ 0 & 0 & 0 & 0 & 1 & 0 & 0 & x & y & 0 & -x^2 & -2x^3y \\ 0 & 0 & 0 & 0 & 2x & 2y + 2 & 2x & 2y & y & 2x & 0 & 0 \end{bmatrix}$
	Displacement interpolation matrix	$N_s = \begin{bmatrix} 1 & 0 & -y & x & \frac{x^2}{2} & y^2 + y & xy & \frac{y^2}{2} & \frac{y^2}{2} & 0 & xy^2 & x^2y^3 \\ 0 & 1 & x & 0 & x^2 + y & x & \frac{x^2}{2} & xy & \frac{y^2}{2} & x^2 & -x^2y & -x^3y^2 \\ 0 & 0 & 1 & 0 & x & -y & 0 & 0 & -\frac{y}{2} & x & -2xy & -3x^2y^2 \end{bmatrix}$
	Geometric matrix	Same as Table 18

5.7 Rebiai, Saidani, and Bahloul (2015- Third quadrilateral element)

In the following of his previous researches, Rebiai, Saidani, and Bahloul [51] suggested another strain-based quadrilateral element for linear dynamic analysis of the plane problems. They utilized the general form of the strain field, which was used in their previous studies, but with slight modifications (see Table 20). The element geometry and its strain state and nodal displacement vectors were similar to the previous element proposed by Rebiai and Beloumar [50]. The difference between these two membrane elements was in their strain and displacement interpolation matrices. Application of this new element for dynamic analysis of the plane problems proved acceptable accuracy of the assumed strain method for the dynamic problems. They utilized the lumped mass matrix for the element.

Table 20: Details of the quadrilateral element proposed by Rebiai, Saidani, and Bahloul [51]

Ref	Properties	
Rebiai et al. [51]	Geometry	Same as Table 18
	Strain field	$\begin{cases} \varepsilon_x(x, y) = (\varepsilon_x)_o + (\varepsilon_y)_o + (\varepsilon_{x,y})_o y + (\varepsilon_y)_o x + (\varepsilon_{x,yy})_o y^2 \\ \quad + 2(\varepsilon_{x,xyyy})_o xy^3 \\ \varepsilon_y(x, y) = (\varepsilon_y)_o + (\varepsilon_{y,x})_o x + (\varepsilon_{y,y})_o y - (\varepsilon_{x,yy})_o x^2 \\ \quad - 2(\varepsilon_{x,xyyy})_o yx^3 \\ \gamma_{xy}(x, y) = 2(\gamma_{xy})_o + [2(\gamma_{xy})_o + 2(\varepsilon_{y,x})_o + (\varepsilon_{y,y})_o] y \\ \quad + 2[(\varepsilon_{x,y})_o + (\varepsilon_y)_o + (\gamma_{xy,x})_o] x \end{cases}$
	Strain state vector	$S = \{u_o \quad v_o \quad r_o \quad (\varepsilon_x)_o \quad (\varepsilon_y)_o \quad (\gamma_{xy})_o \quad (\varepsilon_{x,y})_o \quad (\varepsilon_{y,x})_o \\ (\varepsilon_{y,y})_o \quad (\gamma_{xy,x})_o \quad (\varepsilon_{x,yy})_o \quad (\varepsilon_{x,xyyy})_o\}^T$
	Nodal displacement vector	Same as Table 18
	Strain interpolation matrix	$B_s = \begin{bmatrix} 0 & 0 & 0 & 1 & x + 1 & 0 & y & 0 & 0 & 0 & y^2 & 2xy^3 \\ 0 & 0 & 0 & 0 & 1 & 0 & 0 & x & y & 0 & -x^2 & -2x^3y \\ 0 & 0 & 0 & 0 & 2x & 2y + 2 & 2x & 2y & y & 2x & 0 & 0 \end{bmatrix}$
	Displacement interpolation matrix	$N_s = \begin{bmatrix} 1 & 0 & -y & x \frac{x^2}{2} + x & y^2 + y & xy & \frac{y^2}{2} & \frac{y^2}{2} & 0 & xy^2 & x^2y^3 \\ 0 & 1 & x & 0 & x^2 + y & x & \frac{x^2}{2} & xy & \frac{y^2}{2} & x^2 & -x^2y & -x^3y^2 \\ 0 & 0 & 1 & 0 & x & -y & 0 & 0 & -\frac{y}{2} & x & -2xy & -3x^2y^2 \end{bmatrix}$
Geometric matrix	Same as Table 18	

5.8 Rezaiee-Pajand and Yaghoobi (2015- fourth quadrilateral element)

In most of these formulations, there is no rational basis for the selection of the assumed strain field. However, Rezaiee-Pajand and his colleagues proposed application of the concept of Taylor expansion for this purpose. In an attempt to develop second order strain-based elements, Rezaiee-Pajand and Yaghoobi [67] suggested the complete second-order strain field (see Table 21). Excluding these dependent coefficients from the total strain states, fourteen independent strain states were remained. Accordingly, in this element, the four vertex nodes had three degrees of freedom, namely two displacement and one in-plane rotation, and the internal node had two translational degrees of freedom.

5.9 Rezaiee-Pajand and Yaghoobi (2015- fifth quadrilateral element)

Rezaiee-Pajand and Yaghoobi also proposed another second-order element, in which the assumed strain field was the same as the one presented in Table 21. In addition, the equilibrium criteria were imposed only on the linear terms of the strain components [67]. Therefore, only two strain states were characterized as dependent ones, and eighteen independent strain states remained. To generate an element with eighteen degrees of freedom, they considered a nine-node generalized quadrilateral element, which is demonstrated in Table 22. Each node of this element had two translational degrees of freedom.

5.10 Hamadi, Ayoub, and Maalem (2016)

In 2016, Hamadi, Ayoub, and Maalem [31] independently proposed a new quadrilateral finite element. This element is indeed the same as the element previously proposed by Rezaiee-Pajand and Yaghoobi [63], restricted to rectangular shapes.

5.11 Rezaiee-Pajand and Yaghoobi (2018- sixth quadrilateral elements)

In order to analyze geometrically nonlinear plane structures, Rezaiee-Pajand and Yaghoobi [63] modified their five-node quadrilateral element by the corotational approach [70]. Their findings showed that the strain-based formulation can provide accurate results for geometrically nonlinear analysis of structures. Besides, it did not show any sensitivity to the aspect ratio and mesh distortion. To sum up, the summary of the reviewed elements is presented in Table 23.

6 Other types of strain-based elements

Since the focus of the present study is on the membrane elements, only the available strain-based elements were reviewed in the previous sections. However, the advantages of strain formulation persuade researchers to have taken advantage of this approach in the development of finite elements for other types of structures. In order to provide a brief introduction to the application of assumed strain technique for the proposition of the different finite

Table 21: Details of the fourth quadrilateral element proposed by Rezaiee-Pajand and Yaghoobi [67]

Ref	Properties	
Rezaiee-Pajand and Yaghoobi [67]	Geometry	
	Strain field	$\begin{cases} \varepsilon_x(x, y) = (\varepsilon_x)_o + (\varepsilon_{x,x})_o x + (\varepsilon_{x,y})_o y + (\varepsilon_{x,xx})_o \frac{x^2}{2} \\ \quad + (\varepsilon_{x,xy})_o xy + (\varepsilon_{x,yy})_o \frac{y^2}{2} \\ \varepsilon_y(x, y) = (\varepsilon_y)_o + (\varepsilon_{y,x})_o x + (\varepsilon_{y,y})_o y + (\varepsilon_{y,xx})_o \frac{x^2}{2} \\ \quad + (\varepsilon_{y,xy})_o xy + (\varepsilon_{y,yy})_o \frac{y^2}{2} \\ \gamma_{xy}(x, y) = (\gamma_{xy})_o + (\gamma_{xy,x})_o x + (\gamma_{xy,y})_o y + (\gamma_{xy,xx})_o \frac{x^2}{2} \\ \quad + (\varepsilon_{x,xy} + \varepsilon_{y,xx})_o xy + (\gamma_{xy,yy})_o \frac{y^2}{2} \end{cases}$
	Strain state vector	$S = \{u_o \quad v_o \quad r_o \quad (\varepsilon_x)_o \quad (\varepsilon_y)_o \quad (\gamma_{xy})_o \quad (\varepsilon_{x,x})_o \quad (\varepsilon_{x,y})_o \quad (\varepsilon_{y,x})_o \quad (\varepsilon_{y,y})_o \quad (\varepsilon_{x,xy})_o \quad (\varepsilon_{x,yy})_o \quad (\varepsilon_{y,xy})_o \quad (\varepsilon_{y,xx})_o\}^T$
	Nodal displacement vector	$D = \{D_{3i-2} \quad D_{3i-1} \quad D_{3i} \quad D_{3j-2} \quad D_{3j-1} \quad D_{3j} \quad D_{3k-2} \quad D_{3k-1} \quad D_{3k} \quad D_{3l-2} \quad D_{3l-1} \quad D_{3l} \quad D_{2m-1} \quad D_{2m}\}^T$
	Strain interpolation matrix	$B_s = \begin{bmatrix} 0 & 0 & 0 & 1 & 0 & 0 & 0 & 0 & 0 & 0 & 0 & 0 & 0 & 0 \\ 0 & 0 & 0 & 1 & 0 & 0 & 0 & 0 & 0 & 0 & 0 & 0 & 0 & 0 \\ 0 & 0 & 0 & 0 & 0 & 1 & 0 & 0 & 0 & 0 & 0 & 0 & 0 & 0 \\ 0 & 0 & 0 & 0 & 0 & 0 & 0 & 0 & 0 & 0 & 0 & 0 & 0 & 0 \\ 0 & 0 & 0 & 0 & 0 & 0 & 0 & 0 & 0 & 0 & 0 & 0 & 0 & 0 \\ 0 & 0 & 0 & 0 & 0 & 0 & 0 & 0 & 0 & 0 & 0 & 0 & 0 & 0 \\ 0 & 0 & 0 & 0 & 0 & 0 & 0 & 0 & 0 & 0 & 0 & 0 & 0 & 0 \\ 0 & 0 & 0 & 0 & 0 & 0 & 0 & 0 & 0 & 0 & 0 & 0 & 0 & 0 \\ 0 & 0 & 0 & 0 & 0 & 0 & 0 & 0 & 0 & 0 & 0 & 0 & 0 & 0 \\ 0 & 0 & 0 & 0 & 0 & 0 & 0 & 0 & 0 & 0 & 0 & 0 & 0 & 0 \\ 0 & 0 & 0 & 0 & 0 & 0 & 0 & 0 & 0 & 0 & 0 & 0 & 0 & 0 \\ 0 & 0 & 0 & 0 & 0 & 0 & 0 & 0 & 0 & 0 & 0 & 0 & 0 & 0 \\ 0 & 0 & 0 & 0 & 0 & 0 & 0 & 0 & 0 & 0 & 0 & 0 & 0 & 0 \end{bmatrix}$
	Displacement interpolation matrix	$N_s = \begin{bmatrix} 1 & 0 & -y & x & 0 & \frac{y^2}{2} & -\frac{2G+\lambda}{2G} y^2 & xy & -\frac{2G+\lambda}{2G} y^2 & 0 & \frac{x^2 y}{2} & -\frac{2G+\lambda}{6G} y^2 & \frac{x^2 x}{2} & -\frac{G}{12G+\lambda x^2} & -\frac{G+\lambda}{6G} y^2 & -\frac{G+\lambda}{12G+\lambda x^2} x^2 & -\frac{G}{4G+2\lambda} y^2 & \frac{x^2}{2} & -\frac{G}{4G+2\lambda} y^2 \\ 0 & 1 & x & 0 & y & \frac{x^2}{2} & 0 & -\frac{2G+\lambda}{2G} x^2 & xy & \frac{x^2}{2} & -\frac{2G+\lambda}{6G} x^2 & -\frac{2G+\lambda}{6G} x^2 & -\frac{G+\lambda}{6G} x^2 & -\frac{G+\lambda}{12G+\lambda x^2} y^2 & -\frac{G+\lambda}{12G+\lambda x^2} x^2 & -\frac{G}{12G+\lambda x^2} y^2 & xy & \frac{x^2}{2} & -\frac{G}{4G+2\lambda} y^2 \end{bmatrix}$
	Geometric matrix	$A = [N_{si} \quad T_{si} \quad N_{sj} \quad T_{sj} \quad N_{sk} \quad T_{sk} \quad N_{sl} \quad T_{sl} \quad N_{sm}]^T$ $T_s = [0 \quad 0 \quad 1 \quad 0 \quad 0 \quad \frac{2G+\lambda}{2G} y - \frac{y^2}{2} - \frac{2G+\lambda}{2G} x \quad \frac{y}{2} + \frac{2G+\lambda}{2G} y - \frac{2G+\lambda}{2G} x - \frac{2G+\lambda}{4G} (y^2 - x^2) - \frac{xy}{2} - \frac{2G+\lambda}{4G} (x^2 - y^2) \quad \frac{xy}{2}]$

elements, a short review of the other works is presented in this section. Needless to say, for more details, it is necessary to refer to the original references, which are cited in the following paragraphs.

In the case of plate bending analysis, Belouar and Guenfoud [15] proposed a four-node rectangular plate element by assumption of linear curvature and second-order shear strains. The assumed strain field for the element only satisfies the compatibility condition. They showed that this element is more efficient than the corresponding displacement-based element. In 2014, Hamadi et al. [30] developed a rectangular element for plate bending analysis, based on the Kirchhoff theory, and compared its performance with the

Table 22: Details of the fifth element proposed by Rezaiee-Pajand and Yaghoobi [67]

Ref	Properties	
	Geometry	
Rezaiee-Pajand and Yaghoobi [67]	Strain field	Same as Table 21
	Strain state vector	$S = \{u_o \quad v_o \quad r_o \quad (\varepsilon_x)_o \quad (\varepsilon_y)_o \quad (\gamma_{xy})_o \quad (\varepsilon_{x,x})_o \quad (\varepsilon_{x,y})_o \quad (\varepsilon_{y,x})_o \quad (\varepsilon_{y,y})_o \quad (\varepsilon_{x,xx})_o \quad (\varepsilon_{x,xy})_o \quad (\varepsilon_{x,yy})_o \quad (\varepsilon_{y,xx})_o \quad (\varepsilon_{y,xy})_o \quad (\varepsilon_{y,yy})_o \quad (\gamma_{xy,xx})_o \quad (\gamma_{xy,yy})_o\}^T$
	Nodal displacement vector	$D = \{D_{2i-1} \quad D_{2i} \quad D_{2j-1} \quad D_{2j} \quad D_{2k-1} \quad D_{2k} \quad D_{2l-1} \quad D_{2l} \quad D_{2m-1} \quad D_{2m} \quad D_{2n-1} \quad D_{2n} \quad D_{2p-1} \quad D_{2p} \quad D_{2q-1} \quad D_{2q} \quad D_{2r-1} \quad D_{2r}\}^T$
	Strain interpolation matrix	$B_s = \begin{bmatrix} 0 & 0 & 0 & 1 & 0 & 0 & x & y & 0 & 0 & \frac{x^2}{2} & xy & \frac{y^2}{2} & 0 & 0 & 0 & 0 & 0 & 0 \\ 0 & 0 & 0 & 0 & 1 & 0 & 0 & 0 & x & y & 0 & 0 & 0 & \frac{x^2}{2} & xy & \frac{y^2}{2} & 0 & 0 & 0 \\ 0 & 0 & 0 & 0 & 0 & 1 & -\frac{2G+\lambda}{G}y & -\frac{\lambda}{G}x & -\frac{\lambda}{G}y & -\frac{2G+\lambda}{G}x & 0 & 0 & xy & xy & 0 & 0 & \frac{x^2}{2} & \frac{y^2}{2} \end{bmatrix}$
	Displacement interpolation matrix	$N_s = \begin{bmatrix} 1 & 0 & -y & x & 0 & \frac{y}{2} & \frac{x^2}{2} & -\frac{2G+\lambda}{2G}y^2 & xy & 0 & -\frac{G+\lambda}{2G}y^2 \\ 0 & 1 & x & 0 & y & \frac{x}{2} & 0 & -\frac{G+\lambda}{2G}x^2 & xy & 0 & 0 \\ 0 & 0 & 0 & \frac{x^3}{6} & \frac{x^2y}{2} & \frac{y^2x}{2} & 0 & -\frac{y^3}{6} & 0 & 0 & \frac{y^3}{6} \\ \frac{y^2}{2} & -\frac{2G+\lambda}{2G}x^2 & 0 & -\frac{x^3}{6} & 0 & \frac{x^2y}{2} & \frac{y^2x}{2} & \frac{y^3}{6} & \frac{x^3}{6} & 0 & 0 \end{bmatrix}$
Geometric matrix	$A = [N_{s_i} \quad N_{s_j} \quad N_{s_k} \quad N_{s_l} \quad N_{s_m} \quad N_{s_n} \quad N_{s_p} \quad N_{s_q} \quad N_{s_r}]^T$	

displacement-based formulation. They showed the superiority of strain-based formulation in removing the shear locking problem. Another thin plate element, based on assumed strain approach, is proposed by Abderrahmani, Maalam, and Hamadi [1]. In this study, they utilized higher-order strain field in comparison with the previous elements. In another study, Abderrahmani et al. [2] formulated a new strain-based sector element for linear analysis of circular thin plates in 2017. Many years before this study, another sector strain-based element was proposed by Belarbi and Charif [11]. In 2018, the first triangular plate element, based on assumed strain approach, is proposed by Belounar, Benmebarek, and Belounar [14]. In this study, the

Table 23: Summary of the existing strain-based plane elements reviewed in this article

No.	Element	Geometry	Number of nodes	Number of dof	Assumed strain field			Drilling	Other features
					Normal strain	Shear strain	Optimal criteria		
1	Sabir [71]	Triangular	3	9	Complete linear	Complete linear	Compatibility	yes	-
2	Sabir and Sfendji [72]	Triangular	4	8	Incomplete linear	constant	Compatibility	no	Can be used as transitional element
3	Tayeh [75]	Triangular	3	9	Incomplete second-order	Incomplete second-order	Compatibility	yes	-
4	Belarbi and Bourezane [9]	Triangular	3	9	Complete linear	Incomplete linear	Compatibility	yes	Poisson's ratio is included in the element
5	Belarbi and Bourezane [10]	Triangular	3	9	Incomplete linear	Incomplete second-order	Compatibility	yes	-
6	Rezaiee-Pajand and Yaghoobi [65]	Triangular	6	10	Complete linear	Complete linear	Compatibility Equilibrium	no	Can be used as transitional element
7	Rezaiee-Pajand and Yaghoobi [66]	Triangular	7	10	Complete linear	Complete linear	Compatibility Equilibrium	yes	-
8	Rebiai [48]	Triangular	3	9	Incomplete second-order	Complete second-order	Compatibility	yes	-
9	Rezaiee-Pajand, Gharaei-Moghaddam, and Ramezani [58]	Triangular	5	10	Complete linear	Complete linear	Compatibility Equilibrium	no	Can be used as transitional element
10	Rezaiee-Pajand, Gharaei-Moghaddam, and Ramezani [58]	Triangular	4	10	Complete linear	Complete linear	Compatibility Equilibrium	yes	-
11	Rezaiee-Pajand, Gharaei-Moghaddam, and Ramezani [59]	Triangular	7	11	Complete second-order	Complete linear	Compatibility Equilibrium	yes	-
12	Rezaiee-Pajand, Gharaei-Moghaddam, and Ramezani [61]	Triangular	4	11	Complete second-order	Complete linear	Compatibility Equilibrium	yes	-
13	Rezaiee-Pajand, Ramezani, and Gharaei-Moghaddam [62]	Triangular	7	14	Complete second-order	Complete second-order	Compatibility Equilibrium	yes	-
14	Sabir and Sfendji [72]	Rectangular	5	10	Complete linear	Complete linear	-	no	-
15	Tayeh [75]	Rectangular	4	12	Incomplete fourth-order	Incomplete second-order	Compatibility	yes	-
16	Belarbi and Maalem [12]	Rectangular	5	10	Complete linear	Constant	Compatibility	no	-
17	Rezaiee-Pajand and Yaghoobi [63]	Quadrilateral	5	10	Complete linear	Complete linear	Compatibility Equilibrium	no	-
18	Rezaiee-Pajand and Yaghoobi [64]	Rectangular	5	10	Complete linear	Complete linear	Compatibility Equilibrium	no	-
19	Rezaiee-Pajand and Yaghoobi [64]	Rectangular	5	10	Complete linear	Complete linear	Compatibility Equilibrium	no	Can be used as transitional element
20	Rebiai and Beloumar [49]	Quadrilateral	4	12	Incomplete fourth-order	Complete linear	Compatibility	yes	-
21	Rebiai and Beloumar [50]	Quadrilateral	4	12	Incomplete fourth-order	Complete linear	Compatibility	yes	-
22	Rebiai, Saidani, and Bahloul [51]	Quadrilateral	4	12	Incomplete fourth-order	Complete linear	Compatibility	yes	-
23	Rezaiee-Pajand and Yaghoobi [67]	Quadrilateral	5	14	Complete second-order	Complete second-order	Compatibility Equilibrium	yes	-
24	Rezaiee-Pajand and Yaghoobi [67]	Quadrilateral	9	18	Complete second-order	Complete second-order	Compatibility	yes	-
25	Hamadi, Ayoub, and Maalem [31]	Rectangular	5	10	Complete linear	Complete linear	Compatibility Equilibrium	no	-

authors took an advantage of linear strain components and evaluated the performance of this element in analysis of both thin and thick planes.

One of the first applications of the strain formulation in finite element analysis dates back to 1972 when Ashwell and Sabir [7] proposed a rectangular cylindrical shell element. Later, in 2004, Djoudi and Bahai [24] developed a strain-based shell element, which included openings and cut-outs. They utilized this element to perform vibration analysis of shell structures, and concluded that the strain-based element is more economic than the conventional displacement-based elements. In a comparative study, Hamadi et al. [32] investigated the performance of strain-based shell elements in comparison with the displacement-based elements. This study can be considered an extension of their previous research about plate elements [30]. In 2015, Mousa and Djoudi [45] performed vibration analysis on circular cylindrical shells with oblique ends, by using a new strain-based triangular shell element. For this element, they assumed linear curvature and third-order normal in-plane strains. The most-recent strain-based shell element is a flat triangular hybrid element proposed by Rezaiee-Pajand and Yaghoobi [69]. Trefftz functional was used in this element to formulate independent internal and boundary fields. It must be noted that this work is not the only available hybrid strain-based element and there are other similar studies in the literature. For instance, To and Liu [77] also proposed a triangular shell element, based on the Hellinger-Reissner hybrid strain formulation. Moreover, the hybrid formulation was also utilized for other types of structures. For example, in 2017, Rezaiee-Pajand and Yaghoobi [68] developed a hybrid plane element with assumed strain field.

In addition to the plate and shell element, the assumed strain approach was also utilized for developing three-dimensional finite elements. Belouar and Guerraiche [16] formulated a 3D eight-node brick element by assumption of linear strains. In this formulation, only compatibility criterion was imposed to the assumed strain field. Guerraiche, Belouar, and Bouzidi [29] proposed another variant of this element by using a different assumed strain field. In this new element, they included Poisson's ratio of the material in the strain field of the element. In the most-recent study, Messai, Belouar, and Merzouki [44] suggested a nine-node brick element with linear assumed strain field. In one of the most recent studies in this field, Rezaiee-Pajand, Gharaei-Moghaddam, and Ramezani [60] utilized strain-based formulation and developed a cracked plain element for analysis of cracked structures with open stable cracks.

7 Discussion and conclusion

In this article, which is the first part of a two-part study, the basic formulation steps of the assumed strain approach for developing plane elements were presented. In addition, twenty-five of the available strain-based membrane elements were reviewed, using the unified notations. The reviewed elements

were categorized into two groups of triangular and quadrilateral elements. According to the available literature, most of the accessible elements were formulated by using strain fields, which do not satisfy the equilibrium equations. Moreover, in many of these elements, the assumed strain field seems to be resulted from the trial-and-error process. Because no clear justification was provided by the authors for their selections. Despite this fact, in some cases, especially the elements proposed by Rezaiee-Pajand and his colleagues, the concept of Taylor expansion was considered in the selection of assumed strain components, and in many of these elements, both compatibility and equilibrium criteria were imposed. It is known for the researchers that utilizing incomplete polynomials for strain field might lead to incapability of the element to include Poisson's effect of strain states. Therefore, in some cases the authors tried to consider those strain fields with complete polynomial approximation. It is worth mentioning that the other elements, which do not consider this limitation, can also provide accurate results.

According to the presented review and in some cases, the same elements were proposed by different authors, independently. Therefore, this is one of the main motivations of the present study to provide a comprehensive reference to be used by authors, which helps prevent such duplicate element formulation. In addition, it seems that most of the researchers who worked in this field only followed their own research line and did not take advantage of the other's experiences. Accordingly, there are many unanswered questions about the performance of the strain-based elements that remain to be answered. For instance, it is widely known that some patterns for distribution of the element degrees of freedom resulted in the singular geometric matrix, which was shown by A . In addition, it was concluded that distribution of the degrees of freedom between the element nodes had a considerable effect on the element performance. Despite these indications, it is not clear how to prevent this problem and choose an optimal configuration. Due to these warnings, the application of the higher-order strain fields for membrane elements requires further investigation. According to these points, in the second part of this study, extensive numerical investigations will compare the performance of the reviewed membrane elements.

References

1. Abderrahmani, S., Maalam, T. and Hamadi, D. *On improved thin plate bending rectangular finite element based on the strain approach*, International Journal of Engineering Research in Africa(27) 76–86, Trans Tech Publications, 2016.
2. Abderrahmani, S., Maalem, T., Zatar, A. and Hamadi, D. *A new strain based sector finite element for plate bending problems*, International Jour-

- nal of Engineering Research in Africa (31) 1–13, Trans Tech Publications, 2017.
3. Alsafadie, R., Hjiiaj, M. and Battini, J.M. *Three-dimensional formulation of a mixed corotational thin-walled beam element incorporating shear and warping deformation*, Thin-Walled Struct. 49(4) (2011), 523–533.
 4. Andelfinger U. and Ramm E. *EAS-elements for two-dimensional, three-dimensional, plate and shell structures and their equivalence to HR-elements*, Int. J. Num. Meth. Eng. 36(8) (1993), 1311–1337.
 5. Ansari, S.U., Hussain, M., Mazhar, S., Manzoor, T., Siddiqui, K.J., Abid, M. and Jamal, H. *Mesh partitioning and efficient equation solving techniques by distributed finite element methods: A survey*, Arch. Comput. Methods Eng. 26(1) (2019), 1–16.
 6. Arregui-Mena, J.D., Worth, R.N., Hall, G., Edmondson, P.D., Giorla, A.B. and Burchell, T.D. *A review of finite element method models for nuclear graphite applications*, Arch. Comput. Methods Eng. 27(1) (2020), 331–350.
 7. Ashwell, D.G. and Sabir, A.B. *A new cylindrical shell finite element based on simple independent strain functions*, Int. J. Mech. Sci. 14(3) (1972), 171–183.
 8. Awrejcewicz, J., Krysko, A.V., Zhigalov, M.V. and Krysko, V.A. *Size-Dependent Theories of Beams, Plates and Shells*, Mathematical Modelling and Numerical Analysis of Size-Dependent Structural Members in Temperature Fields 142 (2021) 25–78. Springer, Cham.
 9. Belarbi, M.T. and Bourezane, M., *On improved Sabir triangular element with drilling rotation*, Rev. eur. génie civ., 9(9-10) (2005), 1151–1175.
 10. Belarbi, M.T. and Bourezane, M. *An assumed strain based on triangular element with drilling rotation*, Courier de Savoir, 6 (2005), 117–123.
 11. Belarbi, M.T. and Charif, A. *Nouvel élément secteur basé sur le modèle de déformation avec rotation dans le plan*. Revue Européenne des Éléments Finis, 7(4) (1998), 439–458 (In French).
 12. Belarbi, M.T. and Maalem, T. *On improved rectangular finite element for plane linear elasticity analysis*, Revue Européenne des Éléments Finis, 14(8) (2005), 985–997.
 13. Belarbi, M.O., Zenkour, A.M., Tati, A., Salami, S.J., Khechai, A. and Houari, M.S.A. *An efficient eight- node quadrilateral element for free vibration analysis of multilayer sandwich plates*, Int. J. Num. Meth. Eng. 122(9) (2021), 2360–2387.

14. Belouнар, A., Benmebarek, S. and Belouнар, L. *Strain based triangular finite element for plate bending analysis*, Mech. Adv. Mater. Struct. 27 (8) (2018), 1–13.
15. Belouнар, L. and Guenfoud, M. *A new rectangular finite element based on the strain approach for plate bending*, Thin-Walled Struct., 43(1) (2005), 47–63.
16. Belouнар, L. and Guerraiсhe, K. *A new strain-based brick element for plate bending*, Alex. Eng. J. 53(1) (2014), 95–105.
17. Belytschko, T. and Bindeman, L.P. *Assumed strain stabilization of the eight node hexahedral element*, Comput. Methods Appl. Mech. Eng. 105(2) (1993), 225–260.
18. Bergan, P.G. and Felippa, C. *A triangular membrane element with rotational degrees of freedom*, Comput. Methods Appl. Mech. Eng. 50(1) (1985), 25–69.
19. Bergan, P.G. and Nygård, M.K. *Finite elements with increased freedom in choosing shape functions*, Int. J. Num. Meth. Eng. 20(4) (1984), 643–663.
20. Boutagougа D. *A new enhanced assumed strain quadrilateral membrane element with drilling degree of freedom and modified shape functions*, Int. J. Num. Meth. Eng. 110(6) (2017), 573–600.
21. Chyzy, T. and Mackiewicz, M. *Special finite elements with adaptive strain field on the example of one-dimensional elements*, Appl. Sci. 11(2) (2021), 609.
22. Cinefra, M., de Miguel, A.G., Filippi, M., Houriet, C., Pagani, A. and Carrera, E. *Homogenization and free-vibration analysis of elastic meta-material plates by Carrera Unified Formulation finite elements*, Mech. Adv. Mater. Struct. 28(5) (2021), 476–485.
23. De Souza, R.M. *Force-based finite element for large displacement inelastic analysis of frames* Doctoral dissertation, University of California, Berkeley, 2000.
24. Djoudi, M.S. and Bahai, H. *Strain based finite element for the vibration of cylindrical panels with openings*, Thin-Walled Struct. 42(4) (2004), 575–588.
25. Dow, J.O., Cabiness, H.D. and Ho, T.H. *Linear strain element with curved edges*, J. Struct. Eng. 112(4) (1986), 692–708.
26. Felippa C.A. *A study of optimal membrane triangles with drilling freedoms*, Comput. Methods Appl. Mech. Eng. 192(16-18) (2003), 2125–2168.

27. Felippa C.A. and Militello C. *Membrane triangles with corner drilling freedomsII. The ANDES element*, Finite Elem. Anal. Des. **12**(3-4) (1992), 189-201.
28. Gal, E. and Levy, R. *Geometrically nonlinear analysis of shell structures using a flat triangular shell finite element*, Arch. Comput. Methods Eng. **13**(3) (2006), 331-388.
29. Guerraiche, K., Beloumar, L. and Bouzidi, L. *A new eight nodes brick finite element based on the strain approach*, J. Solid Mech. **10**(1) (2018), 186-199.
30. Hamadi, D., Abderrahmani, S., Maalem, T. and Temami, O. *Efficiency of the Strain Based Approach Formulation for Plate Bending Analysis*, World Academy of Science, Engineering and Technology, International Journal of Mechanical, Aerospace, Industrial, Mechatronic and Manufacturing Engineering, **8**(8) (2014), 1408-1412.
31. Hamadi, D., Ayoub, A. and Maalem, T. *A new strain-based finite element for plane elasticity problems*, Engineering Computations, **33**(2) (2016), 562-579.
32. Hamadi, D., Temami, O., Zatar, A. and Abderrahmani, S. *A Comparative Study between Displacement and Strain Based Formulated Finite Elements Applied to the Analysis of Thin Shell Structures*, World Academy of Science, Engineering and Technology, International Journal of Civil, Environmental, Structural, Construction and Architectural Engineering, **8**(8) (2014), 875-880.
33. Hughes, T.J., Taylor, R.L. and Kanoknukulchai, W. *A simple and efficient finite element for plate bending*, Int. J. Num. Meth. Eng. **11**(10) (1977), 1529-1543.
34. Jafari, V., Vahdani, S.H. and Rahimian, M. *Derivation of the consistent flexibility matrix for geometrically nonlinear Timoshenko frame finite element*, Finite Elem. Anal. Des. **46**(12) (2010), 1077-1085.
35. Jang, J. and Pinsky, P.M. *An assumed covariant strain based 9-node shell element*, Int. J. Num. Meth. Eng. **24**(12) (1987), 2389-2411.
36. Khorsandnia, N., Valipour, H., Foster, S. and Crews, K. *A force-based frame finite element formulation for analysis of two-and three-layered composite beams with material non-linearity*, Int. J. NonLinear Mech. **62** (2014), 12-22.
37. Korelc J. and Wriggers, P. *Improved enhanced strain four-node element with Taylor expansion of the shape functions*, Int. J. Num. Meth. Eng. **40**(3) (1997), 407-421.

38. Kwan, A.K.H. *Analysis of buildings using strain-based element with rotational DOFs*, J. Struct. Eng. 118(5) (1992), 1191–1212.
39. Li, L.X., Chen, Y.L. and Lu, Z.C. *Generalization of the multi-scale finite element method to plane elasticity problems*, Appl. Math. Model. 39(2) (2015), 642–653.
40. Logg, A. *Automating the finite element method*, Arch. Comput. Methods Eng. 14(2) (2007), 93–138.
41. Manta, D., Gonçalves, R. and Camotim, D. *Combining shell and GBT-based finite elements: Plastic analysis with adaptive mesh refinement*, Thin-Walled Struct. 158 (2021), 107205.
42. Marras, S., Kelly, J.F., Moragues, M., Müller, A., Kopera, M.A., Vázquez, M., Giraldo, F.X., Houzeaux, G. and Jorba, O. *A review of element-based Galerkin methods for numerical weather prediction: Finite elements, spectral elements, and discontinuous Galerkin*, Arch. Computat. Methods Eng. 23 (4) (2016), 673–722.
43. Meier, C., Popp, A. and Wall, W.A. *Geometrically exact finite element formulations for slender beams: Kirchhoff–Love theory versus Simo–Reissner theory*, Arch. Comput. Methods Eng. 26(1) (2019), 163–243.
44. Messai, A., Belounar, L. and Merzouki, T. *Static and free vibration of plates with a strain-based brick element*, Eur. J. Comput. Mech. (2019), 1–21.
45. Mousa, A. and Djoudi, M. *New strain based triangular finite element for the vibration of circular cylindrical shell with oblique ends*, Int. J. Civ. Environ. Eng. 15(5) (2015), 6–11.
46. Neuenhofer, A. and Filippou, F.C. *Evaluation of nonlinear frame finite-element models*, J. Struct. Eng. 123(7) (1997), 958–966.
47. Neuenhofer, A. and Filippou, F.C. *Geometrically nonlinear flexibility-based frame finite element*, J. Struct. Eng. 124(6) (1998), 704–711.
48. Rebiai, C. *Finite element analysis of 2-D structures by new strain based triangular element*, J. Mech. (2018), 1–9.
49. Rebiai, C. and Belounar, L. *A new strain based rectangular finite element with drilling rotation for linear and nonlinear analysis*, Archives of civil and mechanical engineering, 13(1) (2013), 72–81.
50. Rebiai, C. and Belounar, L. *An effective quadrilateral membrane finite element based on the strain approach*, Measurement, 50 (2014), 263–269.
51. Rebiai, C., Saidani, N. and Bahloul, E. *A New Finite Element Based on the Strain Approach for Linear and Dynamic Analysis*, Research Journal of Applied Sciences, Engineering and Technology, 11(6) (2015), 639–644.

52. Reddy, J.N. *An introduction to the finite element method*, (Vol. 2, No. 2.2). New York: McGraw-hill, 1993.
53. Rezaiee-Pajand, M., Arabi, E. and Moradi, A.H. *Static and dynamic analysis of FG plates using a locking free 3D plate bending element*, J. Braz. Soc. Mech. Sci. Eng. 43(1) (2021), 1–12.
54. Rezaiee-Pajand, M. and Gharaei-Moghaddam, N. *Analysis of 3D Timoshenko frames having geometrical and material nonlinearities*, Int. J. Mech. Sci. 94 (2015), 140–155.
55. Rezaiee-Pajand, M. and Gharaei-Moghaddam, N. *Frame nonlinear analysis by force method*, Int. J. Steel Struct. 17(2) (2017), 609–629.
56. Rezaiee-Pajand, M. and Gharaei-Moghaddam, N. *Vibration and static analysis of cracked and non-cracked non-prismatic frames by force formulation*, Eng. Struct. 185 (2019), 106–121.
57. Rezaiee-Pajand, M. and Gharaei-Moghaddam, N. *Force-based curved beam elements with open radial edge cracks*, Mech. Adv. Mater. Struct. 27(2) (2020), 128–140.
58. Rezaiee-Pajand, M., Gharaei-Moghaddam, N. and Ramezani, M. *Two triangular membrane element based on strain*, Int. J. Appl. Mech. 11(1) (2019), 1950010.
59. Rezaiee-Pajand, M., Gharaei-Moghaddam, N. and Ramezani, M.R. *A new higher-order strain-based plane element*, Scientia Iranica. Transaction A, Civil Engineering, 26(4) (2019), 2258–2275.
60. Rezaiee-Pajand, M., Gharaei-Moghaddam, N. and Ramezani, M., *Strain-based plane element for fracture mechanics' problems*, Theor. Appl. Fract. Mech. 108 (2020), 102569.
61. Rezaiee-Pajand, M., Gharaei-Moghaddam, N. and Ramezani, M., *Higher-order assumed strain plane element immune to mesh distortion*, Eng. Comput. 37(9) (2020), 2957–2981.
62. Rezaiee-Pajand, M., Ramezani, M. and Gharaei-Moghaddam, N. *Using higher-order strain interpolation function to improve the accuracy of structural responses*, Int. J. Appl. Mech. 12(3) (2020), 2050026.
63. Rezaiee-Pajand, M. and Yaghoobi, M. *Formulating an effective generalized four-sided element*, Eur. J. Mech. A Solids, 36 (2012), 141–155.
64. Rezaiee-Pajand, M. and Yaghoobi, M. *A free of parasitic shear strain formulation for plane element*, Research in Civil and Environmental Engineering, 1 (2013) 1–27.

65. Rezaiee-Pajand, M. and Yaghoobi, M. *A robust triangular membrane element*, Lat. Am. J. Solids Struct. 11(14) (2014), 2648–2671.
66. Rezaiee-Pajand, M. and Yaghoobi, M. *An efficient formulation for linear and geometric non-linear membrane elements*, Lat. Am. J. Solids Struct. 11(6) (2014), 1012–1035.
67. Rezaiee-Pajand, M. and Yaghoobi, M. *Two new quadrilateral elements based on strain states*, Civ. Eng. Infrastruct. J., 48(1) (2015), 133–156.
68. Rezaiee-Pajand, M. and Yaghoobi, M. *A hybrid stress plane element with strain field*, Civ. Eng. Infrastruct. J. 50(2) (2017), 255–275.
69. Rezaiee-Pajand, M. and Yaghoobi, M. *An efficient flat shell element*, Meccanica, 53(4-5) (2018), 1015–1035.
70. Rezaiee-Pajand, M. and Yaghoobi, M. *Geometrical nonlinear analysis by plane quadrilateral element*, Scientia Iranica, 25(5) (2018), 2488–2500.
71. Sabir, A.B. *A rectangular and triangular plane elasticity element with drilling degrees of freedom*, In Proceedings of the Second International Conference on Variational Methods in Engineering, Brebbia CA ed., Southampton University (1985), 17–25.
72. Sabir, A.B. and Sfindji, A. *Triangular and rectangular plane elasticity finite elements*, Thin-Walled Struct. 21(3) (1995), 225–232.
73. Saritas, A. and Filippou, F.C. *Inelastic axial-flexure-shear coupling in a mixed formulation beam finite element*, Int. J. Non Linear Mech. 44(8) (2009), 913–922.
74. Spacone, E., Ciampi, V. and Filippou, F.C. *Mixed formulation of nonlinear beam finite element*, Comput. Struct. 58 (1) (1996), 71–83.
75. Tayeh, S.M. *New strain-based triangular and rectangular finite elements for plane elasticity problems*, Thesis, The Islamic University, Gaza, 2003.
76. Taylor, R.L., Filippou, F.C., Saritas, A. and Auricchio, F. *A mixed finite element method for beam and frame problems*, Comput. Mech. 31(1) (2003), 192–203.
77. To, C.W.S. and Liu, M.L. *Hybrid strain based three-node flat triangular shell elements*, Finite Elem. Anal. Des., 17(3) (1994), 169–203.
78. Xu, M., Gitman, I.M. and Askes, H. *A gradient-enriched continuum model for magneto-elastic coupling: Formulation, finite element implementation and in-plane problems*, Comput. Struct. 212 (2019), 275–288.
79. Yang, H.T., Saigal, S., Masud, A. and Kapania, R.K. *A survey of recent shell finite elements*, Int. J. Num. Meth. Eng. 47(1a3) (2000), 101–127.

80. Zienkiewicz O.C. and Taylor R.L. *The finite element method for solid and structural mechanics*, Elsevier, 2005.